Cellulose (2022) 29:5943–5977
https://doi.org/10.1007/s10570-022-04660-0

REVIEW PAPER

Hydrophobization of lignocellulosic materials part III: modification with polymers

Sandra Rodríguez-Fabià · Jonathan Torstensen · Lars Johansson · Kristin Syverud

Received: 24 January 2022 / Accepted: 19 May 2022 / Published online: 16 June 2022

Abstract This review is the third part of a series of reviews on hydrophobization of lignocellulosic materials, a relevant topic nowadays, due to the need to replace fossil fuel-based materials. The review provides an overview of the hydrophobization of lignocellulosic materials by polymer adsorption, and both chemical and radiation-induced grafting of polymers. While adsorbed polymers are only attached to the surfaces by physical interactions, grafted polymers are chemically bonded to the materials. Radiation-induced grafting is typically the most environmentally friendly grafting technique, even though it provides little control on the polymer synthesis. On the other hand, controlled radical polymerization reactions are more complex but allow for the synthesis of polymers with elaborated architectures and well-defined properties. Overall, a wide range of contact angles can be obtained by polymer adsorption and grafting, from a slight increase in hydrophobicity to superhydrophobic properties. The choice of modification technique depends on the end-use of the modified material, but there is a clear trend towards the use of more environmentally friendly chemicals and processes and the grafting of polymers with complex structures.

Graphical abstract

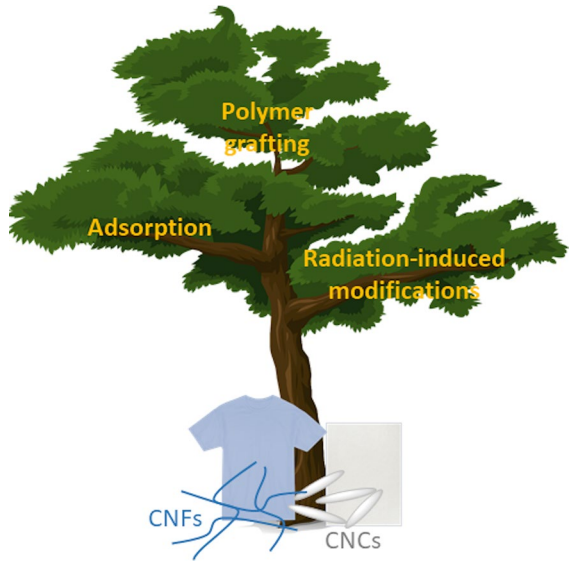

Keywords Cellulose · Hydrophobization · Polymer grafting · Polymer adsorption

S. Rodríguez-Fabià (✉) · L. Johansson · K. Syverud
RISE PFI, Trondheim, Norway
e-mail: sandra.fabia@rise-pfi.no

J. Torstensen
Western Norway University of Applied Sciences, Bergen, Norway

K. Syverud
Department of Chemical Engineering, NTNU, Trondheim, Norway

Introduction

The recent directive from the European Union on the ban of single-use plastics has opened the market for cellulose-based products (EU 2019). Cellulosic materials have been widely investigated due to the abundance and availability of cellulose as a raw material. The growing interest in sustainable materials to replace fossil fuel-based products has positioned lignocellulosic materials in the form of fibers, cellulose nanocrystals (CNCs), and cellulose nanofibrils (CNFs) as one of the most promising alternatives, particularly in application areas such as packaging and single-use plastic products.

Lignocellulosic materials are found in wood, plants, vegetables, seaweed and algae, and they are mostly constituted of cellulose, hemicelluloses and lignin (Chen 2014). Cellulose is the most abundant biopolymer and in addition to being found in lignocellulosic materials, it is also produced by bacteria and tunicates. Cellulose is a linear polymer formed by D-glucopyranose rings linked by β-(1→4) glycosidic bonds, resulting in a sequence of anhydroglucose units (glucose residues) that, at least in the neat cellulose crystal structures, are rotated 180° with respect to each other (Fig. 1). Each AGU has three available hydroxyl groups that form a network of hydrogen bonds and van der Waals interactions that result in the self-assembly of cellulose chains into elementary/native fibrils, which contain both crystalline and amorphous domains. The degree of crystallinity is dependent on the cellulose source. The structure of the elementary fibril is specie dependent and debated (Jarvis 2018). Models where 18 cellulose molecules are combined into an elementary fibril have been proposed, although packing of 24 is also possible (Purushotham et al. 2020). Fibrils are combined into microfibrils, where they are packed together with lignin and hemicelluloses. These microfibrils are in turn packed into cellulose fibers (Dufresne 2013).

Cellulosic nanomaterials can be isolated from cellulose fibers. These materials are called nanocelluloses and have at least one dimension in the nanometer range. Cellulose fibers can be disintegrated into CNFs by mechanical treatment, although the fibers often undergo a chemical or enzymatic pre-treatment in order to facilitate the process. CNFs form a web-like structure and contain both amorphous and crystalline domains. On the other hand, CNCs are highly crystalline rods that are typically obtained by acid hydrolysis. Depending on the acid used, the surface charge and nanocrystal properties may vary. The last type of nanocelluloses is bacterial nanocellulose (BNC). BNC is produced by anaerobic bacteria of the genus *Gluconacetobacter* and forms a 3D network of nanofibrils (Klemm et al. 2011; Habibi 2014).

Cellulose and nanocelluloses are amphiphilic (Medronho and Lindman 2014), but to fully exploit the potential of these materials it is often necessary to modify their properties, for example, by increasing their hydrophobicity. Hydrophobization of (nano)celluloses is an important tool to develop new sustainable materials used in, for example, oil absorption (Laitinen et al. 2017), composite materials (Habibi et al. 2008; Kedzior et al. 2016), membrane separation (Dizge et al. 2019), or (food) packaging (Rodionova et al. 2011; Balasubramaniam et al. 2020). As mentioned earlier, the glucose residues composing the cellulose molecules have three available hydroxyl groups. The ability of cellulose to form hydrogen bonds allows molecules to adsorb onto the surface of cellulose. In addition to hydrogen bonding, these

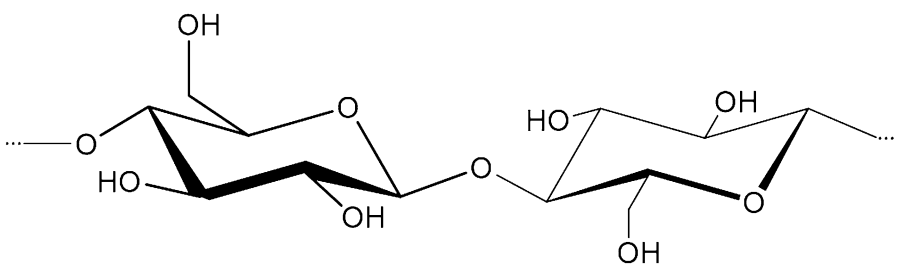

Fig. 1 Chemical structure of cellulose, where glucose is the repeating unit. Two glucose residues are shown for clarity. Note that the left glucose residue is drawn in the standard viewing position with the C5-O5 bond at the back, somewhat higher on the page than the C2-C3 bond

functional groups can be used to chemically modify the properties of the (nano)fibers. Common chemical modification methods include esterification, silylation, click-chemistry, and polymer grafting.

There are many reviews describing methods for the modification of celluloses. However, only a few of them are focused on the hydrophobization of these materials or in the modification with polymers (Roy et al. 2009; Cunha and Gandini 2010). This review is the third part of a series of three reviews about the hydrophobization of lignocellulosic materials. In this review, we present a comprehensive compilation of modifications of cellulosic materials with polymers, by both physical adsorption and grafting.

Hydrophobization techniques

Hydrophobization of (nano)celluloses is a field of high interest that encompasses many different modification approaches. For instance, there are physical modification methods such as adsorption of molecules and polymers or plasma etching (*Hydrophobization of lignocellulosic materials part I: physical modification*) (Rodríguez-Fabià et al. 2022), and also grafting of molecules by a wide variety of reactions such as esterification, etherification, and silylation (*Hydrophobization of lignocellulosic materials part II: chemical modification*). In addition to grafting and adsorption of "short" molecules, grafting and adsorption of polymers are also techniques used to modify cellulosic materials. This review solely focuses on modification methods with polymers, either by adsorption or grafting of the polymer itself or by polymerization of a monomer at the surface of the substrate. The modification of lignocellulosic materials can occur either at the surface of the substrate or in bulk. In the case of modifications with polymers, it is safe to assume that the modification occurs only at the surface of the substrates. Clearly, adsorption of polymers takes place at the surface of the material, but also grafting reactions start from activated sites located at the surface of the substrate.

Hydrophobization of cellulosic materials usually requires the extensive use of solvents such as water and organic solvents such as, for example, tetrahydrofuran and dimethylformamide (Kedzior et al. 2019). Relevant modification methods are layer by layer deposition (Forsman et al. 2020), electrospinning (Kalantari et al. 2018), as well as dip-coating, deposition of nanoparticles and grafting of hydrophobic molecules (Wei et al. 2020). In terms of simplicity and applicability, one-pot processes that only require cellulose, solvent (preferably water) and the hydrophobing agent are desirable. With regards to polymeric modifications, organic solvents are commonly used in both "grafting to" and "grafting from" approaches. Larger hydrophobic polymers used in the "grafting to" approach are not water-soluble, which is also true for most monomers used in the "grafting from" approach. The development of water-based "grafting from" reactions is receiving more and more attention, with more complex, multi-step methods for water-based reactions (Zoppe et al. 2017). It should however be noted that in the case of nanocellulose modification, modified species will agglomerate in water as the hydrophobing modification proceeds. In the case of polymer adsorption, the polymers are often dispersed in water in the form of nanoparticles (Nurmi et al. 2010) or dissolved in water when the polymers are polyelectrolytes (Ogawa et al. 2007). Moreover, adsorbed polyelectrolyte multilayers can act as binders for the adsorption of nanoparticles onto cellulosic substrates (Ogawa et al. 2007; Forsman et al. 2017).

Possible methods to evaluate (ligno)cellulosic hydrophobicity include contact angle (CA) measurements, water vapour transmission rate (WVTR), water vapour swelling and the water vapour retention value (WRV). Other methods include hydrophobic polymer compatibility for (nano)composites. As discussed in (Rodríguez-Fabià et al. 2022), lignocellulosic materials readily sorb water, and thus, the contact angle, water vapor transmission rate, water vapour swelling and water vapour retention value are material and history dependent. In terms of evaluating the contact angle, this is typically done immediately upon droplet deposition. As time proceeds the contact angle will decline as the droplet is being sorbed (Dankovich and Gray 2011). Thus, a larger, more stable contact angle is regarded as a measure of hydrophobicity. It should here be noted that the contact angle is also affected by the surface nano and micro-structure. However, in most studies the detected contact angle for lignocellulosic materials is typically $< 50°$ (Atalla et al. 1980; Dankovich and Gray 2011; Abitbol et al. 2014). Most hydrophobization studies aim at achieving CAs $> 90°$, and the effect

of the surface treatments on the contact angle can be easily differentiated from variations in contact angles of neat lignocellulosic materials. However, it should be noted that most authors do not separate the contribution of modified surface chemistry from the original surface properties of the substrate.

Grafting of polymers may be evaluated in terms of visible surface modifications or the degree of grafting, which is typically expressed as the grafting yield (G, 1) or the grafting efficiency (G_E, 2):

$$G = \frac{m_G}{m_{Cell}} \cdot 100 \quad (1)$$

$$G_E = \frac{m_G}{m_G + m_P} \cdot 100 \quad (2)$$

where m_G is the mass of the grafted polymer, m_{Cell} is the mass of cellulose, and m_P is the mass of homopolymer.

Techniques such as atomic force microscopy (AFM) (Lönnberg et al. 2006; Ahmadi et al. 2017) or scanning electron microscopy (SEM) (Roy et al. 2005) are typically employed to reveal morphological changes to the material surface. The presence of substitution may be investigated by attenuated total reflection Fourier-transform infrared (ATR-FTIR) (Kelly et al. 2021), nuclear magnetic resonance (NMR) (Olsén et al. 2020), Raman spectroscopy (Zhu et al. 2021), elemental analysis (Roy et al. 2005), gravimetrically (Ahmadi et al. 2017) or by time-of-flight secondary ion mass spectrometry (ToF–SIMS) (Yang et al. 2011; Ahmadi et al. 2017). In Roy et al. (2005), Lönnberg et al. (2006), Ahmadi et al. (2017) and Kelly et al. (2021), some of these methods are also used to determine the degree of grafting. Of these techniques, only ToF–SIMS is a true surface technique with a surface penetration depth of ca. 2 nm (Ahmadi et al. 2017). However, when the degree of polymeric substitution is determined by other methods it is typically assumed to be on the surface. One notable exception is polymer grafting in combination with swelling (Olsén et al. 2020), where bulk substitution is achieved. For molecular hydrophobization, unchanged crystallinity is often used as an indication of surface substitution, while a decrease in crystallinity indicates bulk and surface substitution (Çetin et al. 2009; Guo et al. 2017). This method is however impossible to apply in polymer grafting, as grafted polymers are partially amorphous, thus decreasing the material crystallinity, regardless of the location of the substitution.

Adsorption

Adsorption of polymers onto cellulosic materials is a non-covalent modification method driven by hydrogen bonding, van der Waals and electrostatic interactions, and the affinity between functional groups and surface structure (Rechendorff et al. 2006; Habibi 2014; Hubbe 2015). Several methods can be used to coat surfaces with polymers, such as layer-by-layer deposition, dip-coating, and electro-spraying. These polymers can be amphiphilic copolymers, polyelectrolytes, or hyperbranched polymers. Moreover, the effect of polymer coatings has been enhanced by combining polymer deposition with the adsorption of solid particles and additional fluorinated coatings.

Cellulosic filter paper surfaces were coated with either statistical copolymers or block copolymers of 2,2,2-trifluoroethyl methacrylate (TFEMA) and 2-(dimethylamino)ethyl methacrylate (DMAEMA) (Nurmi et al. 2010). Polymer nanoparticles were prepared by solvent exchange from acetone to water, which were adsorbed onto the surfaces as dispersed aqueous nanoparticles in an aqueous solution. The hydrodynamic diameter (D_H) of the nanoparticles was in the range 60–82 nm at pH 6.5. The filter paper was immersed in the nanoparticle suspension during 10 min, followed by immersion and thorough rinsing with water. The substrates were either dried at ambient conditions or annealed. Only the annealed filter paper surfaces modified with the statistical copolymer C-51 (51% TFEMA, P(TFEMA$_{75}$-co-DMAEMA$_{73}$), M_n = 24,100 g/mol, polydispersity index (PDI) = 1.24, D_H = 64 nm) and the block copolymer B-77 (77% TFEMA, PTFEMA$_{107}$-b-P(DMAEMA$_{36}$-co-TFEMA$_{22}$), M_n = 27,300 g/mol, PDI = 1.40, D_H = 60 nm) did not absorb water and presented advancing contact angles of 160°. The receding contact angles were uneven, presenting values between 0 and 120°. The hydrophobic behaviour is caused by two different factors: the roughness of the paper surface and the polymer properties.

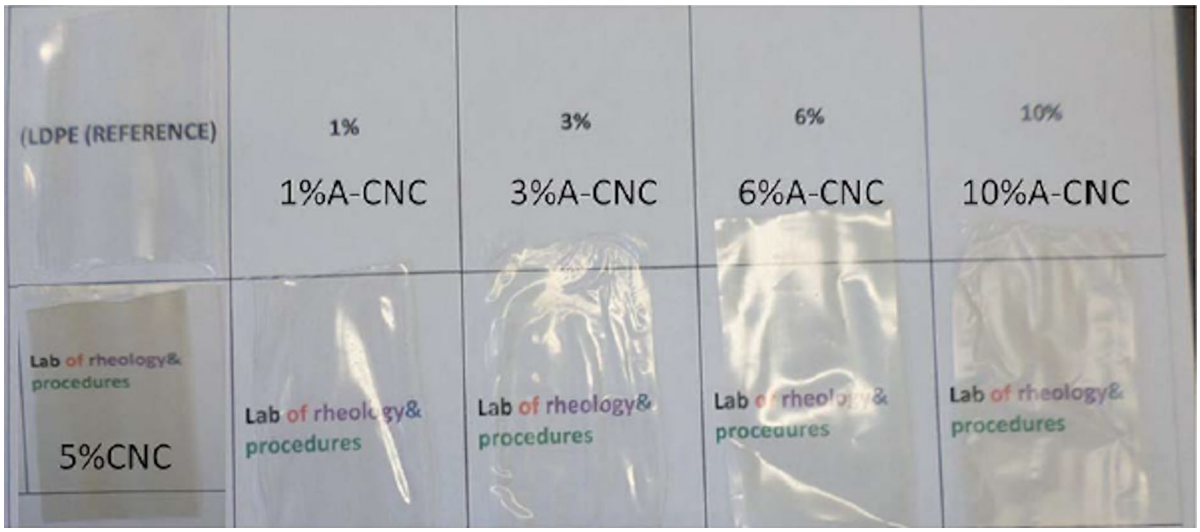

Fig. 2 Comparison of extruded polyethylene films containing CNCs and CNCs with adsorbed PEO-PPO-PEO (A-CNC). Image reproduced from Nagalakshmaiah et al. (2016)

Amphiphilic triblock copolymers of poly(ethylene oxide)-poly(propylene oxide)- poly(ethylene oxide) (PEO-PPO-PEO), available under the trade name Pluronics, have been used in composite materials to improve the dispersion of cellulosic materials. CNCs were coated with PEO-PPO-PEO, providing improved compatibility between the CNCs and a polyethylene matrix, as well as the mechanical and thermal properties (Nagalakshmaiah et al. 2016). The resulting nanocomposite films obtained by extrusion are displayed in Fig. 2. The image shows the improved transparency of films containing adsorbed CNCs (A-CNCs) compared with a film containing CNCs, caused by an enhanced distribution of the A-CNCs within the polymer matrix and improved thermal properties of these composites.

Two different PEO-PPO-PEO copolymers (commercial name Pluronic L61: $M_w = 2000$ g/mol, $PEO_2PPO_{30}PEO_2$; commercial name Pluronic L121: $M_w = 4400$ g/mol, PEO_4–PPO_{69}–PEO_4) were used in epoxy composites reinforced with cellulose nanowiskers (CNWs). Composites with Pluronic L61 displayed better mechanical properties than epoxy, epoxy/CNW composites and epoxy/CNW-L121 composites, which suggest that this surfactant provides better coverage of the CNWs (Emami et al. 2015).

Cotton fabric was coated with 10 different kinds of hyperbranched fluorinated polymers which were either derivatives of hyperbranched polyesters (degree of branching (DB) = 0.47–0.57, $M_n = 5100$–$15{,}100$ g/mol and PDI = 1.01–1.04) or hyperbranched poly(urea-urethane) (DB = 0.43, $M_n = 32{,}500$ g/mol and PDI = 5.27) (Tang et al. 2010). The contact angles of these samples ranged from 139 to 146°. Moreover, the polymers modified with 1H,1H,2H,2H-perfluorooctanol presented also lipophobic properties. The contact angles of n-hexadecane and n-decane on cotton surfaces coated with these polymers ranged from 119 to 122° and 94 to 102°, respectively. The samples fluorinated with 1H,1H,2H,2H-perfluorooctanol displayed the highest water repellency ratings, showing that these samples had outstanding hydrophobicity for impacting droplets.

The hydrophobing effect of polymer coatings has been enhanced by combining polymer deposition with the adsorption of solid particles and additional modification with fluorinated compounds. For example, cellulose acetate nanofibrous membranes were modified with fluoroalkylsilane (FAS) in order to mimic the superhydrophobic surfaces of silver ragwort leaves (Ogawa et al. 2007). The surface of the negatively charged cellulose acetate fibers was first coated with alternating layers of TiO_2 nanoparticles (30% aqueous suspension, diameter = 7 nm) and poly acrylic acid (PAA, $M_w = 90{,}000$ g/mol), and then with FAS (Fig. 3). The membranes were immersed in a 0.1 wt% TiO_2 solution at pH 2.5 for 15 min, rinsed with water and then immersed in a 10^{-2} M PAA solution

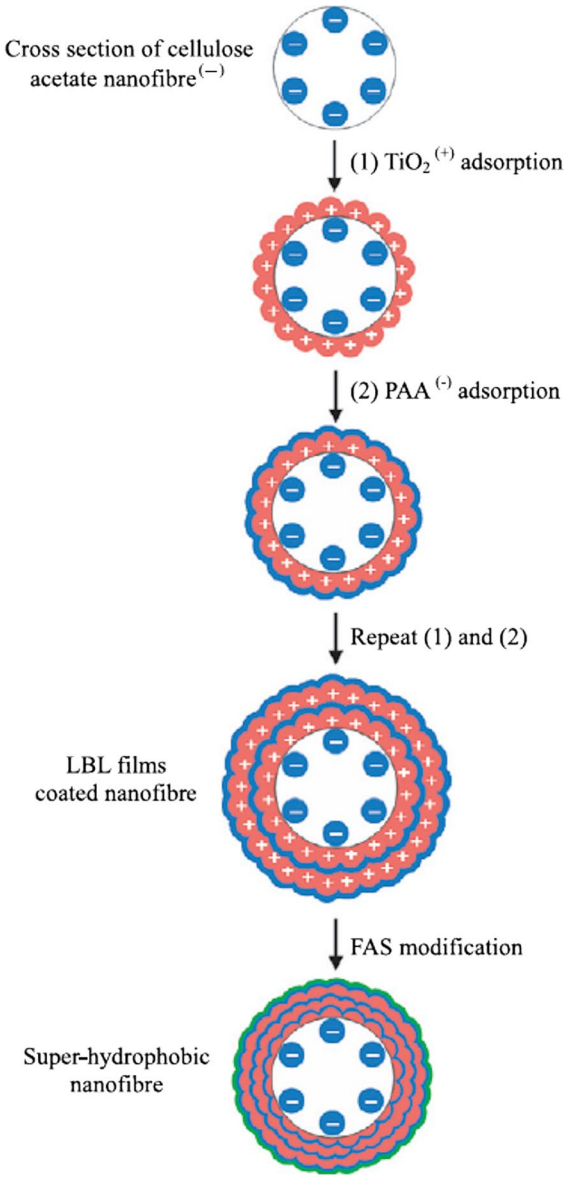

Fig. 3 Schematic representation of the preparation of superhydrophobic surfaces by layer-by-layer deposition of TiO_2 and PAA followed by FAS coating. Image reproduced from (Ogawa et al. 2007)

at pH 2.5 for 15 min, followed by rinsing with water. This process was repeated several times and then the dry membranes were immersed in a 3 wt% FAS solution for 6 h. This treatment provided the fibers with a super-hydrophobic coating (FAS) and with surface roughness characteristics of silver ragwort leaves. The highest contact angles were obtained on fiber films with coatings of 5 and 10 TiO_2/PAA bilayers and a FAS coating, achieving super-hydrophobicity with contact angles of 154 and 162°, respectively, while the contact angle of FAS-coated fibers was 138°. Overall, the hydrophobicity of the samples increased with increasing surface roughness.

The same approach was used to obtain superhydrophobic paper by deposition of alternating layers of poly(diallyldimethylammonium chloride) (PDADMAC, molecular weight: 100,000–200,000 g/mol) and silica particles (diameters: 220 nm, 420 nm, 680 nm, and 1 µm), followed by a hydrophobic coating of 1H,1H,2H,2H-perfluorooctyltriethoxysilane (POTS) (Yang and Deng 2008). The silica particles were synthesized by hydrolysis of tetraethyl orthosilicate in presence of catalytic amounts of NH_4OH. The reaction was performed at room temperature over a period of two days. Linerboard from unbleached kraft softwood fibers was used as substrate. To obtain super-hydrophobic a surface, the paper was immersed in a PDADMAC solution for 20 min, rinsed with water, followed by immersion in a silica aqueous suspension for 10 min, and then rinsed again with water. Then the coated surface was coated with POTS via chemical vapour deposition. The contact angles of the untreated paper, hydrophobic paper (HP, only coated with POTS), and super-hydrophobic paper (SHP, coated with PDADMAC/silica particles (220 nm) and POTS) were 51°, 110° and 155°, respectively. Moreover, the effect of the silica particles size was investigated, showing that the larger the particle size, the lower the contact angle. Hydrophobic paper and super-hydrophobic paper presented much lower moisture content and higher tensile strength than untreated paper. The water contact angle of SHP samples remained above 150° after immersing the substrates in water. In addition, the increasing hydrophobicity of the substrates strongly hindered bacterial growth.

Forsman et al. (2017) used layer-by-layer deposition to coat CNF films and cotton and linen fabrics with poly-l-lysine (PLL, molecular weight: 150,000–300,000 g/mol) and wax particles. The wax dispersion was prepared by addition of wax to water at 90 °C followed by sonication. The wax dispersion was cooled down and filtered through a filter with 100–160 µm pore size. The substrates were immersed for 5 min in solutions with concentrations of 10 mg/l for PLL and 10 g/l for wax. The substrates were thoroughly rinsed with water after the adsorption of each

layer. After coating the CNF films with a PLL/wax bilayer, the water contact angle increased from 34° to 94°, and after two bilayers it reached 138°. The steep increase in contact angle was partly caused by an increase in surface roughness by the wax particles. Annealing of the sample coated with one bilayer increased the contact angle due to the better spreading of the coating, while it decreased the contact angle of the sample coated with two bilayers due to loss of surface roughness. Regarding cotton and linen samples, the water contact angle of coated cotton was 140° and increased to 156° after annealing. Coated linen had a contact angle of 146°, which decreased to 139° after annealing.

Wood fibers were coated with two different types of polyelectrolyte multilayers (PEMs) (Lingström et al. 2007). The initial advancing contact angle was between 15° and 40°. The first type of coating was a combination of poly allylamine (PAH)/PAA and the second one was a combination of PEO/PAA. Fibers coated with PAH/PAA reached steady state after 4–5 polymer layers at pH 5. When PAH was at the topmost layer, the advancing contact angle oscillated between 72 and 77°, whereas when PAA was at the topmost layer the contact angles ranged between 35° and 40°. At pH 7.5/3.5, stability was reached after 2–3 layers and yielded advancing contact angles between 101° and 107° when PAH was adsorbed at the top layer, and between 40° and 50° when PAA was at the top layer. Coatings of PEO/PAA did not present significant variations in the advancing contact angle depending on which polymer was adsorbed at the topmost layer. After adsorption of two layers, all contact angles oscillated between 45 and 60°. The contact angle measurements also showed a correlation between the wettability of the surfaces and the mechanical properties, where the coatings with the highest advancing contact angles also presented increasing tensile indexes.

Further research was performed on layer-by-layer deposition of PAH and PAA in combination with commercial emulsion of anionic paraffin wax, to increase the hydrophobicity of softwood kraft pulp fibers (Gustafsson et al. 2012). Polymer solutions of 30 mg/g fiber were added separately to a 4 g/l fiber. The polymers were allowed to adsorb for 20 min and then the fibers were rinsed with water. Adsorption of PAH was performed at pH 7.5 and adsorption of PAA at pH 3.5. After adsorption of 2.5 bilayers (three layers of a PAH layer and two of PAA), wax particles were adsorbed onto the fibers for 20 min (3, 15 or 30 mg wax/g fiber added to a 4 g/l fiber suspension at pH 8.5), and sheets from the PEM-modified fibers were immediately prepared. The tensile strength and strain at break of the sheets were improved by the PEM coating, but they decreased in the case of wax-coated sheets. Regarding the contact angle measurements, both the wax treatment and curing of the samples had a positive effect in increasing the hydrophobicity of the substrates. The sample with only polymer coating absorbed water before the heat treatment, and afterwards the contact angle was 113°. After wax coating, the highest contact angle (142°) was obtained for the samples with the highest wax content (18.6 mg/g), while after heat treatment, a contact angle of 151° was achieved in samples with 8.1 mg/g of wax.

Sakakibara et al. (2016) used amphiphilic diblock copolymers of poly(lauryl methacrylate)-block-poly(2-hydroxyethyl methacrylate) (PLMA-PHEMA, $M_{n\ PLMA\ block} = 7.0 \times 10^3$ g/mol, $M_{n\ PLMA\text{-}b\text{-}PHEMA} = 8.8 \times 10^3$ g/mol, PDI = 1.3) to facilitate the dispersion of CNFs in high-density polyethylene resin. The contact angle of modified CNF films increased from 48 to 101°. The improved dispersibility of the coated CNFs resulted in an increase of 140% in the Young's modulus of the reinforced high-density polyethylene resins, as well as an increase of 84% in the tensile strength.

An overview of the modifications by polymer adsorption is given in Table 1.

Polymer grafting

Modification of cellulosic materials can also be achieved by grafting polymers. Often, polymer grafting is used in composite materials to improve the compatibility of the filler with the polymer matrix. Two different approaches are used for grafting of polymers onto surfaces: "grafting to" and "grafting from", illustrated in Fig. 4. In the "grafting to" approach, pre-synthesized polymer chains with reactive end-groups are attached to the cellulose substrates, allowing to characterize the polymers before grafting and control the properties of the resulting material. This approach is typically used for

Table 1 Overview of modifications of cellulosic materials by adsorption

Source of cellulose	Type of cellulose	Polymer	Contact angle (°)	References
Filter paper	Cellulose fibers	TFEMA-st-DMAEMA, TFEMA-b-DMAEMA,	Advancing CA: 160 Receding CA: 0–120	Nurmi et al. (2010)
	CNC	PEO-PPO-PEO	–	Emami et al. (2015), Nagalakshmaiah et al. (2016)
Cotton fabric	Cotton fabric	Hyperbranched polyesters, hyperbranched poly(urea-urethane)	139–146	Tang et al. (2010)
	Cellulose acetate nanofibers	TiO_2 nanoparticles/PAA + FAS	5 TiO_2/PAA bilayers + FAS: 154 10 TiO_2/PAA bilayers + FAS: 162 FAS: 138	Ogawa et al. (2007)
Linerboard from unbleached kraft softwood pulp	Wood fibers	PDADMAC/silica particles + POTS	HP: 110 SHP (220 nm): 155 SHP (420 nm): 152 SHP (680 nm): 150 SHP (1000 nm): 145	Yang and Deng (2008)
Never-dried bleached hardwood kraft pulp	CNF	PLL + wax	CNF 1 bilayer: 94 CNF 2 bilayers: 138	Forsman et al. (2017)
	Cotton fabric Linen fabric		Cotton: 140 Cotton annealed: 156 Linen: 146 Linen annealed: 139	
Chlorine-free bleached chemical softwood fibers	Wood fibers	PAH/PAA PEO/PAA	pH 5: PAH/PAA: 72–77, 35–40 * pH 7.5/3.5: PAH/PAA: 101–107, 40–50 * PEO/PAA: 45–60	Lingström et al. (2007)
Unbeaten, once-dried, virgin softwood kraft pulp fibers	Wood fibers	PAH/PAA + wax	PAH/PAA cured: 113 PAH/PAA + wax: 142 PAH/PAA + wax cured: 151	Gustafsson et al. (2012)
Needle-leaf bleached kraft pulp	CNF	PLMA-PHEMA	101	Sakakibara et al. (2016)

*The first value range corresponds to samples with PAH at the outermost layer and the second value range to samples with PAA at the outermost layer

lignocellulosic fibers or CNCs and results in low grafting densities due to the steric hindrance caused by the already grafted polymer chains, which prevents the diffusion of new chains towards the surface. On the other hand, in the "grafting from" approach, the polymer chains are grown at the surface of the substrate, using the hydroxyl groups directly as initiating sites or after activation. This method allows for high grafting densities, although the properties of the grafted polymer chains are not well defined and are difficult to control. A more detailed review about modification of CNCs through polymer grafting was published by Kedzior et al. (2019). The findings discussed in this section for the "grafting to" approach are summarized in Table 2, and the findings for the "grafting from" approach are summarized in Table 3.

Grafting to

In the "grafting to" strategy, polymers are tethered to the cellulosic substrates, typically cellulose fibers and CNCs. Click chemistry is one of the most

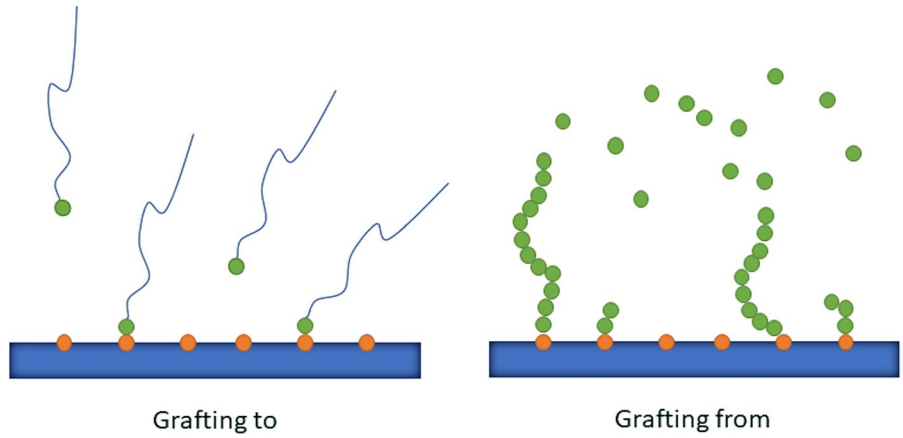

Fig. 4 Schematic representation of the "grafting to" and "grafting from" approaches

Table 2 Overview of modifications of cellulosic materials by "grafting to"

Cellulose source	Type of cellulose	Polymer	Reaction type/covalent bond	Grafting yield (wt.%)	CA (°)	References
	CNC	PCL-diol	Azide alkyne cycloaddition/1,2,3-triazole			(Zhou et al. 2018)
Avicel	Microcrystalline cellulose (MCC)	PCL-diol	Azide alkyne cycloaddition/1,2,3-triazole			(Krouit et al. 2008)
HEC		PLA, (PEG)	Azide alkyne cycloaddition/1,2,3-triazole			(Eissa et al. 2012)
Ramie fibers	CNC	PCL	Bimolecular addition/ urethane bond		64,75	(Habibi and Dufresne 2008)
	CNC	PHBV	Esterification/ester bond		46–60	(Yu and Qin 2014)
	CNC	PS, poly(*tert*-butyl acrylate)	Amidation reaction/ amide bond	60–64		(Harrisson et al. 2011)
Cotton	CNC	Polyether-polyurethane prepolymer	Bimolecular addition/ urethane bond			(Pei et al. 2011)
Bleached kraft pulp	Fibers	Maleated polypropylene	Esterification/ ester bond			(Felix et al. 1993)
Cotton fabric	Fibers	PEG5000-*b*-P(MA-*co*-APM)-*b*-PHFA	Azide photolysis/ amine, amide bonds		155	(Li et al. 2010a)
		P(APM-*co*-HFA)			138	
BNC		PLA-co-PGMA	Nucleophilic substitution/ ester bond		51–82	(Li et al. 2010b)
Jute fabric	Fibers	PBA	Free radical coupling (ether, alkane bonds)	2.34–2.98	125.1	(Bao et al. 2020)

used routes to graft polymers. Poly(ε-caprolactone) (PCL) was successfully grafted onto CNCs and cellulose fibers by azide-alkyne cycloaddition reactions (Krouit et al. 2008; Zhou et al. 2018). The hydrophobic CNCs could be dispersed in chloroform

Table 3 Overview of modifications of cellulosic materials by "grafting from"

ROP

Source of cellulose	Type of cellulose	Monomer	Grafting yield (%)	Contact angle (°)	References
Whatman filter paper	Fibers	ε-CL	11	114	(Hafrén and Córdova 2005)
Cotton					
	MFC	ε-CL	16, 19, 21		(Lönnberg et al. 2008)
Oil palm mesocarp fibers	Fibers	ε-CL	78		(Eksiler et al. 2018)
Ramie fibers	CNC	ε-CL		80	(Habibi et al. 2008)
Linter	CNC	ε-CL	85		(Lin et al. 2009)
MCC	CNC	ε-CL	91.7–95.6	72.55–89.01	(Chen et al. 2009)
Ramie fibers	CNC	L-lactide			(Goffin et al. 2011)
Ramie fibers	CNC	D-lactide			(Habibi et al. 2013)
MCC	CNC	L-lactide			(Lizundia et al. 2016)

Free radical polymerization

Source of cellulose	Type of cellulose	Initiator	Monomer	Grafting yield (%)	Grafting efficiency (%)	CA	References
Fully bleached spruce sulphite cellulose	MFC	CAN	GMA				(Stenstad et al. 2008)
Bleached birch pulp	CNF	CAN	GMA	146–439	96–99		(Littunen et al. 2011)
			Ethyl acrylate	95–255	0–85		
			MMA	56–98	56–75		
			Butyl acrylate	177–392	83–89		
			2-hydroxyethyl methacrylate	19–37	18–64		
Cellulose powder		CAN	Ethyl acrylate		54.2–75.6		(Gupta et al. 2002)
Cotton filter	CNC	CAN	MMA	11		34.5	(Kedzior et al. 2016)
Cotton filter	CNC	CAN	4VP			34–47	(Kan et al. 2013)
Hibiscus sabdariffa	Fibers	KPS	MA	8.79–63.15			(Thakur and Singha 2010)
Hibiscus sabdariffa	Fibers	KPS	MMA	5.47–50.93			(Thakur et al. 2011)
Cotton fiber	Fibers	KPS	MA	< 36.5			(Mondal et al. 2008)
			MMA	< 43.1			
			VAc	< 27.4			
MCC powder	CNC	KPS	Styrene			78	(Espino-Pérez et al. 2016)
Bleached softwood kraft pulp	CNF	KPS	BA/styrene			149	(Mulyadi et al. 2016)
Cellulose powder		Fenton	Vinyl acetate	0–12%	0–2.6		(Misra et al. 1979)
Cellulose powder		Fenton	Ethyl acrylate	2.7–345.0	0.42–54.0		(Misra et al. 1980)
Abelmoschus manihot	Fibers	Fenton	MMA	130			(Jadhav and Jadhav 2021)
Bleached eucalyptus pulp	CNF	Fenton	Methacrylic acid, maleic acid	130			(Maatar and Boufi 2015)

Table 3 (continued)

NMP					
Source of cellulose		Type of cellulose	Monomer	Grafting yield (%)	References
Bleached softwood Kraft pulp		CNC	DMAEMA	41.68, 65.18	(Garcia-Valdez et al. 2017)
			DEAEMA	36.08, 53.05	
			DMAPMAm	39.59, 49.13	
Cellulose acetate			Styrene		(Moreira et al. 2015)
ATRP					
Source of cellulose	Type of cellulose	Monomer	Grafting yield (%)	Contact angle (°)	References
Cotton wool	CNC	Styrene	8–22		(Morandi et al. 2009)
Filter paper	CNC	Styrene	68		(Yi et al. 2008)
Filter paper	Fibers	MA		128, 133	(Carlmark and Malmström 2002)
Filter paper*	Fibers	MMA		109–112	(Hansson et al. 2009)
		Styrene		132–137	
		GMA		-	
Filter paper*	Fibers	Lauryl acrylate		125, 135	(Arteta et al. 2017)
		Octadecyl acrylate		134, 146	
Poplar wood*	Wood	MMA	2.36–12.84	74–130	(Fu et al. 2012)
Filter paper	Fibers	GMA		154, 172	(Nyström et al. 2006)
Cotton fabric		GMA		140.1–155, 163.7	(Li et al. 2015)
Norway spruce*	Wood	TFEMA	Pyridine: 43.4 Dichloromethane: 42.9		(Vidiella del Blanco et al. 2019)
Filter paper	Fibers	NIPAAm		110	(Lindqvist et al. 2008)
		GMA/NIPAAm		130	
		4VP		pH 7 = 90–100 pH 9 = 125	
		NiPAAm/4VP		115–120	
	CNF	Styrene	12.7–46.2	85.1–98.7	(Huang et al. 2015)
BNC	BNC	MMA	59–887	134	(Lacerda et al. 2013)
		BA	110	116	
		MMA/BA	616		
RAFT					
Source of cellulose	Type of cellulose	Monomer	Grafting yield (%)	Contact angle (°)	References
MCC	CNC	MMA			(Anžlovar et al. 2016)
Whatman filter paper	CNC	VAc			(Boujemaoui et al. 2016)
Hydroxypropyl cellulose		VAc	69		(Fleet et al. 2008)
Methyl cellulose			61		
Pinus Maritimus natural fibers	Fibers	VAc, BA			(Tastet et al. 2011)
		Styrene		95	
		Styrene/ VBC		~90–95	
Cotton fabric	Fibers	Styrene			(Perrier et al. 2004)
		MA			
		MMA			
Whatman filter paper	Fibers	Styrene	11–28	~130	(Roy et al. 2005)

*ARGET ATRP

but not in water. Another example is the grafting of poly(lactic acid) (PLA) and polyethylene glycol (PEG) onto 2-hydroxyethyl cellulose, yielding hydrophobic and hydrophilic composites, respectively (Eissa et al. 2012). Other examples are the use of isocyanates to graft polymers onto cellulose. PCL with isocyanate end-groups was grafted onto CNCs to use the CNCs as reinforcing materials in PCL/CNC composites (Habibi and Dufresne 2008). Polymers with varying chain lengths were selected, and the contact angle of CNC films increased from 43° to 75°.

Similarly, poly(3-hydroxybutyrate-co-3-hydroxyvalerate) (PHBV) was grafted onto CNCs using 2,4-toluene diisocyanate (TDI) as coupling agent (Yu and Qin 2014). The DS increased with increasing concentration of TDI in the reaction mixture. Grafted CNCs presented contact angles between 46° and 60°, showing that the modified CNCs were more hydrophobic than the unmodified ones (30°).

Cellulose TEMPO-oxidized microcrystals were grafted with polystyrene (PS) and poly(*tert*-butyl acrylate) (Harrisson et al. 2011). The resulting nanorods contained 60–64 wt% grafted polymer and formed stable suspensions in acetone, toluene and chloroform. A similar synthetic approach was used to obtain polyurethane/CNC nanocomposites with remarkable mechanical properties (Pei et al. 2011). A polyether–polyurethane prepolymer was synthesized in the presence of CNCs. Films with varying concentrations of CNCs were prepared by casting and presented high tensile strength and stain-to-failure as well as improved thermal stability.

Cellulose fibers grafted with two different maleated polypropylenes (4500 g/mol and 39,000 g/mol) were used to prepare composites of a commercial polypropylene (Threspaphan NNA 30), PS, and chlorinated polyethylene (Felix et al. 1993). Modification was achieved by adding cellulose fibers to 5 wt% maleated PP dispersed in toluene for 5 min. The surface energies of the low molecular weight and high molecular weight-grafted fibers were 40 and 36.9 mJ/m^2, meaning that the substrates were hydrophobic. Regarding the mechanical properties of the composites, in all cases, those prepared with high molecular weight polypropylene exhibited the best mechanical properties.

The amphiphilic block copolymers poly(ethylene glycol)(5000)-*b*-poly(methyl acrylate-*co*-4-azidophenyl methacrylate)-*b*-poly(2,2,3,4,4,4-hexafluorobutyl acrylate) (PEG5000-*b*-P(MA-*co*-APM)-*b*-PHFA) and P(APM-*co*-HFA) were synthesized, and grafted onto cotton fabric (Li et al. 2010a). Coatings of PEG5000-*b*-P(MA-*co*-APM)-*b*-PHFA resulted in superhydrophobic surfaces with contact angles of 155°, while P(APM-*co*-HFA) rendered contact angles of 138°. The superhydrophobic coatings were further tested, showing that the contact angle remains constant after one month of storage in air. Treatment of this coating in acidic, basic and organic solvents showed that the coating had good chemical stability since it displayed contact angles > 147°.

Graft copolymers of PLA and poly(glycidyl methacrylate) (PLA-co-PGMA) were synthesized and grafted onto bacterial nanocelulose samples which had undergone different pretreatments (Li et al. 2010b). The grafting reaction occurred between the hydroxyl groups in BNC and the epoxydes from the synthetic polymer. A sample of BNC was activated with an aminosilane coupling agent (KH550), and this sample displayed the highest contact angle value (82°), while the remaining samples presented values between 51° and 61°.

Bao et al. (2020) successfully grafted the hydrophobic polymer poly(butyl acrylate) (PBA) from jute fabric. Jute fibers typically have high lignin content, and the grafting was performed between the pre-synthesized polymers and the lignin present in the fibers via enzyme-initiated reversible addition-fragmentation chain transfer polymerization. PBA with four different molecular weights (M_n = 4251–6491 g/mol, PDI = 1.14–1.24) were grafted, and the contact angle of grafted jute fabric increased from 85.7° to 125°.

Grafting from

The modification of cellulosic materials using the "grafting from" approach is an extensive field of growing interest in the past years. The polymerization methods can be divided into three main groups which are: ring-opening polymerization (ROP), free radical polymerization, and controlled radical polymerization.

Ring-opening polymerization (ROP) Ring-opening polymerization is used to graft polymers from cyclic monomers, typically lactones or lactides. The

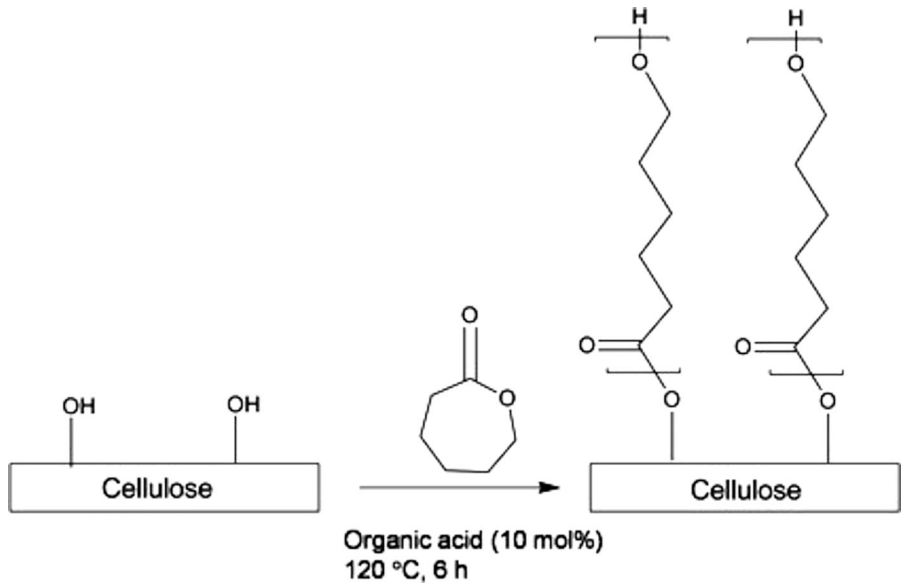

Fig. 5 Schematic representation of ROP with PCL. Image obtained from Carlmark et al. (2012)

hydroxyl groups present at the surface of the cellulosic materials act as initiators for the polymerization reaction. Typically, the polymerization of lactones and lactides is catalyzed by tin (II) 2-ethylhexanoate, which reacts with the hydroxyl groups of cellulose and actually initiates the reaction (Carlmark et al. 2012). This is illustrated in Fig. 5.

Hafrén and Córdova (2005) were the first to graft a polymer to cellulose fibers via metal- and solvent-free surface-initiated ROP (SI-ROP). ε-caprolactone (ε-CL) was grafted from cotton and filter paper by immersing the samples in the monomer/initiator mixture. The catalyst tartaric acid provided the highest degree of grafting, with a weight increase of the paper samples up to 11%. Modified cotton samples did not absorb water and floated when placed on the surface of water-filled cups, contrary to the unmodified cotton fibers, which immediately sank. The water contact angle of the modified paper was 114°. In another example of ROP, ε-CL was grafted from microfibrillated cellulose (Lönnberg et al. 2008). Three different molecular weights of the grafted polymers were targeted. The fractions of PCL in the composites were 16%, 19%, and 21%. The modified MFC had good dispersibility in tetrahydrofuran (THF), indicating an increase in hydrophobicity.

Oil palm mesocarp fibers (OPMFs) were grafted with PCL via vapor-phase-assisted surface polymerization (Eksiler et al. 2018). In this technique, the monomers are in the vapour phase and can penetrate the porous structure of the OPMFs and modify both at the interior and exterior surface of the fibers, resulting in higher grafting yields than the traditional liquid process. The weight of the grafted fibers consisted of 78% PCL (M_w = 12,000 g/mol). Size exclusion chromatography analysis confirmed that the grafting occurred in the hydroxyl groups of cellulose, hemicellulose and lignin. This method has been used to develop surface-modified lignocellulosic nanofibers. After modification, the fibers were milled in presence of an ionic liquid to fibrillate the fibers. The pulverized particles retained the PCL coating, and when dispersed in a PCL matrix, the coated particles were well dispersed.

CNCs were also grafted via ROP with ε-CL (Habibi et al. 2008). The modified CNCs displayed better dispersibility in toluene and had a water contact angle of 80°. These CNCs were used as reinforcing materials for PCL composites and showed improved Young's modulus and storage modulus than PLA and unmodified CNC/PLA composites. ROP of ε-CL on CNC powder has also been performed through microwave irradiation (Chen et al. 2009; Lin et al. 2009). The resulting CNCs were either blended with PCL (Lin et al. 2009) or thermoformed into sheets (Chen et al. 2009). The biocomposites presented enhanced strength and elongation. Sheets made from CNCs grafted with long polymer chains had higher mechanical strength than those with short grafted chains. As a result of grafting, the CNCs became more

hydrophobic and produced sheets with water contact angles between 72° and 89°.

There are several studies where PLA-grafted CNCs are used to increase the compatibility of CNCs in PLA composites (Goffin et al. 2011; Habibi et al. 2013; Lizundia et al. 2016). As an example, Lizundia et al. (2016) grafted CNCs with L-lactide via SI-ROP. The grafted CNCs were dispersed in a PLA matrix to create biocomposites. The mechanical, thermal and optical properties of these composites were affected by the CNC:lactide ratio. The tensile strength of the composites with grafted CNCs improved, while the ductility of the material decreased.

Free radical polymerization Free radical polymerization from cellulosic materials is usually performed in water using water-soluble initiators and monomers. Common initiators are ceric ammonium nitrate (CAN), potassium persulfate (KPS), Fenton's reagent, and ammonium persulfate (APS), although APS has so far only been used for grafting hydrophilic polymers (Kedzior et al. 2019). In free radical polymerization, the initiators generate radicals either by decomposition caused by light or heat (KPS) or by a redox reaction (CAN, Fenton) (Tosh and Routray 2014). The free radical polymerization mechanism consists of three steps: i) initiation, ii) propagation and iii) termination, as illustrated in Fig. 6. In the initiation step, radicals originating from an initiator or radiation (see the *radiation-induced modifications* section) form new radicals on the cellulose molecules by abstraction of hydrogen atoms. These new radicals can attack monomers and form a new covalent bond between cellulose and the monomer (M). The reaction propagates to new monomers, while the polymer chain grafted to the cellulose molecule grows. This is the propagation

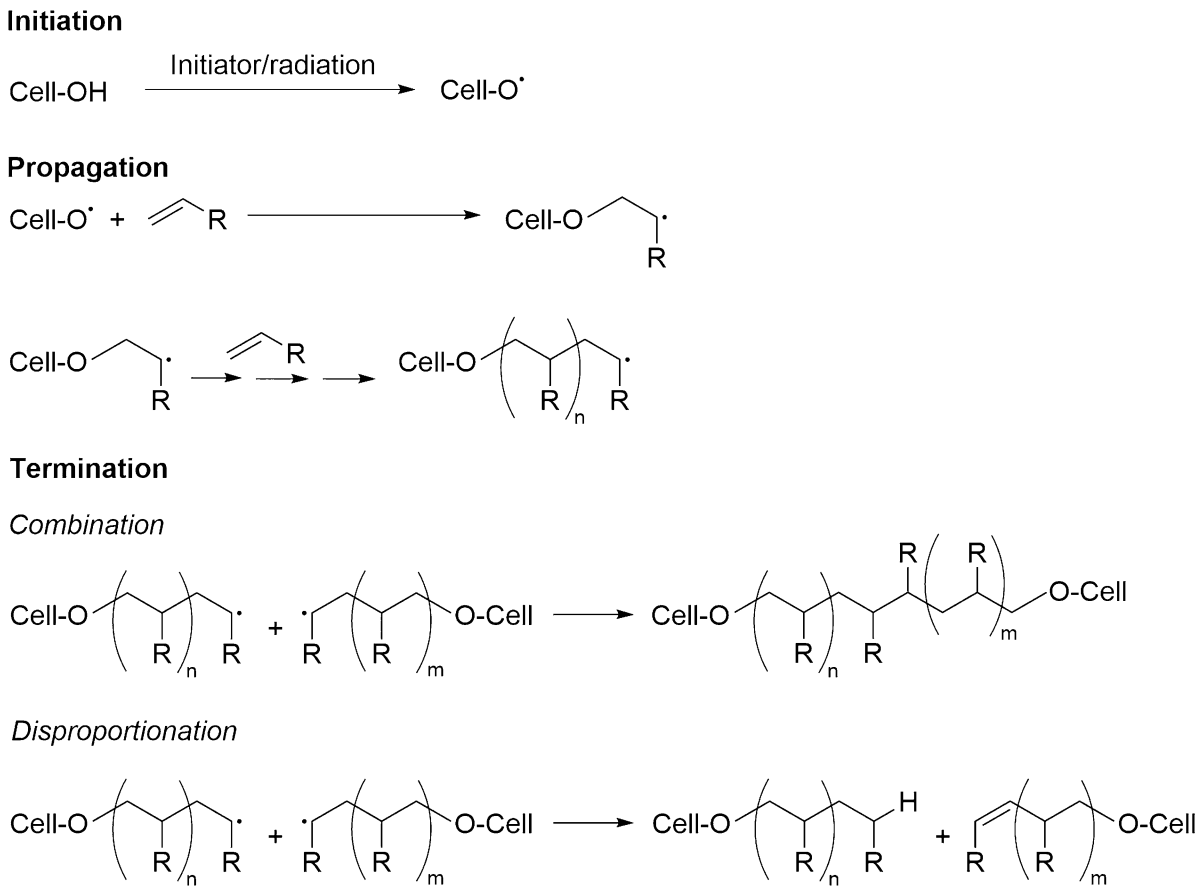

Fig. 6 Mechanism of free radical polymerization of a vinyl monomer from cellulose

step. Finally, the reaction ends either by the combination of two radical chains or by the disproportionation mechanism, where one radical chain abstracts a hydrogen from another one, resulting in a hydrogen-terminated chain, and a chain with a double bond. Additional reactions that can occur but are not shown in the figure are the synthesis of free homopolymer and side reactions such as beta-session of cellulose main-chains, which leads to the molecular weight decrease (Ogiwara and Kubota 1973).

Cerium ammonium nitrate (CAN)

Glycidyl methacrylate (GMA) was grafted from microfibrillated cellulose using CAN as initiator (Stenstad et al. 2008). Grafting with GMA was performed in water with 0.1 M HNO_3. The nanofibrils were successfully coated with brushes of a hydrophobic polymer that contains an epoxy group, which can be used for further modifications. In addition to glycidyl methacrylate, Littunen et al. (2011) also grafted other acrylic monomers (ethyl acrylate, methyl methacrylate, butyl acrylate, and 2-hydroxyethyl methacrylate) from nanofibrillated cellulose. All monomers were successfully grafted, and higher grafting yields than for macroscopic cellulose were achieved. The grafted polymers were hydrolyzed and precipitated in a non-solvent, and then characterized by gel permeation chromatography. Butyl acrylate formed the longest polymers with molecular weights up to 3500 kg/mol, while ethyl acrylate and methyl methacrylate formed polymer chains with molecular weights in the range of 100–400 kg/mol. All the investigated monomers made the grafted CNFs more hydrophobic. Grafting with CAN has also been used to graft ethyl acrylate from cellulose powder (Gupta et al. 2002).

CAN was also employed for grafting of CNCs with poly(methyl methacrylate) (PMMA) (Kedzior et al. 2016). The CNCs had an initial contact angle of 18°. A grafting of 11 wt% was achieved in this study, resulting in CNCs with contact angles of 34.5°. The obtained grafting yield is lower than the typically achieved by controlled radical polymerization, which is between 50 and 92 wt%. PMMA/CNC nanocomposites presented decreased thermal stability compared with pure PMMA. Only the composites with the highest CNC content displayed increased Young's modulus, suggesting that a higher content of CNC is required to obtain a reinforcing effect in the nanocomposites. Poly(4-vinylpyridine) (P4VP) was also grafted from CNCs using CAN as initiator in a one-pot, water-based reaction (Kan et al. 2013). The length of the grafted chains was approximately 150 repeating units, and a grafting of approximately one 4VP repeating unit per every three anhydroglucose units was estimated. The water contact angles of CNC and grafted CNC films were measured at various pH, and the films displayed contact angles between 15°–19° and 34°–47°, respectively. The contact angles of the grafted CNC films increased when the pH was higher than 5, although the increase in the film hydrophobicity was modest.

Potassium persulfate (KPS)

Cellulose fibers were grafted with methyl acrylate (MA) and methyl methacrylate (MMA) (Thakur and Singha 2010; Thakur et al. 2011). Grafting yields of 9–63% and 5–51% were obtained for MA and MMA, respectively. The moisture absorbance of the fibers decreased with increasing grafting percentage, whereas the resistance to acid and basic media increased with the degree of grafting.

Cotton fibers were first scoured with either water or different amine solutions and then grafted with hydrophilic and hydrophobic monomers (Mondal et al. 2008). The hydrophobic monomers were MA, MMA and vinyl acetate (VAc). The highest grafting yields were obtained with water-activated samples and were 36.5%, 41.3% and 27.4% for MA, MMA and VAc. MA and MMA grafted samples displayed the lowest moisture sorption due to the high hydrophobicity of the polymers. The mechanical strength of the fibers remained unchanged after grafting.

CNCs were grafted with polystyrene through a two-step procedure. The CNCs were oxidized by ozonolysis and then styrene was grafted from the activated CNCs (Espino-Pérez et al. 2016). The grafting efficiency was 0.24 molecules of styrene for each AGU. Films of grafted CNCs presented contact angles of 78° and enhanced thermal stability. Grafting improved the compatibility between PLA and the CNCs, and composites of PLA/grafted CNCs resulted in materials with lower vapor permeability than both PLA and PLA/CNCs.

Hydrophobic aerogels were prepared from a CNF suspension modified with *n*-butyl acrylate (BA) and styrene copolymers (Mulyadi et al. 2016). The aerogels achieved almost super-hydrophobic properties, displaying a contact angle of 149°, as well as high absorption of organic solvents. These aerogels

presented similar hydrophobicity and sorption capacity as other aerogels modified with fluorinated compounds, being, therefore, a more environmentally friendly alternative.

Fenton's reagent

Fenton's reagent is based on a Fe^{2+}- H_2O_2 system that generates hydroxyl radicals from the redox reaction that occurs between these two components. The pH plays a crucial role in the formation of free radicals and hence the reaction performance. Misra et al. (1979, 1980) used Fenton chemistry to graft poly(vinyl acetate) (PVAc) and poly(ethyl acrylate) from cellulose. The effect of additives (ascorbic acid, EDTA, potassium fluoride), as well as the ratio between Fe^{2+} and H_2O_2 on the grafting efficiency of both monomers were investigated. Results showed that in both cases none of the tested additives promoted grafting and that the optimal Fe^{2+}/H_2O_2 ratio was 1.04:1. Ethyl acrylate presented higher reactivity than vinyl acetate, resulting in higher grafting efficiencies.

Abelmoschus manihot fibers were modified by grafting PMMA for potential oil absorbency applications (Jadhav and Jadhav 2021). The reaction parameters were optimized to a reaction time of 150 min, 75 °C, monomer to fiber ratio of 3:1, material to liquor ratio of 1:75 and Fe^{2+}/H_2O_2 ratio 20:20. Under these conditions a grafting yield of 130% was obtained and the maximum oil absorbency of crude oil, diesel oil, engine oil and used engine oil was achieved. Additionally, the moisture absorbance and swelling of the fibers in presence of water and ethanol decreased with increasing grafting yield.

A hydrophobic CNF aerogel was prepared by grafting copolymers of methacrylic and maleic acids from the aerogel surface (Maatar and Boufi 2015). A grafting yield of 130% was achieved and the grafted aerogel retained its structural integrity after immersion in water. In addition, the grafted aerogel presented enhanced adsorption of metal ions compared with the unmodified aerogel.

Controlled radical polymerization Controlled radical polymerization allows the synthesis of polymers with defined architecture, composition and molecular weight distribution. Polymers with these characteristics are obtained using reagents that transfer the growing chains to a dormant state that is in equilibrium with the active species. Three types of controlled polymerization are used to graft polymers from cellulosic materials: nitroxide-mediated polymerization (NMP), atom transfer polymerization (ATRP), and reversible addition-fragmentation chain-transfer polymerization (RAFT).

NMP

This polymerization method uses stable nitroxide radicals that react with the growing polymer chains, forming a (macro)alkoxyamine, as shown in Fig. 7. The (macro)alkoxyamine is in a dormant state, which lowers the number of active chains and the possibility of bimolecular chain termination. By increasing the temperature, the nitroxide moiety is cleaved, generating again a propagating chain. The most common reagent used in NMP is TEMPO, although SG1 (*N*-(2-methylpropyl)-*N*-(1-diethylphosphono-2,2-dimethylpropyl)-*N*-oxyl) has been proven to be a more versatile initiator that can

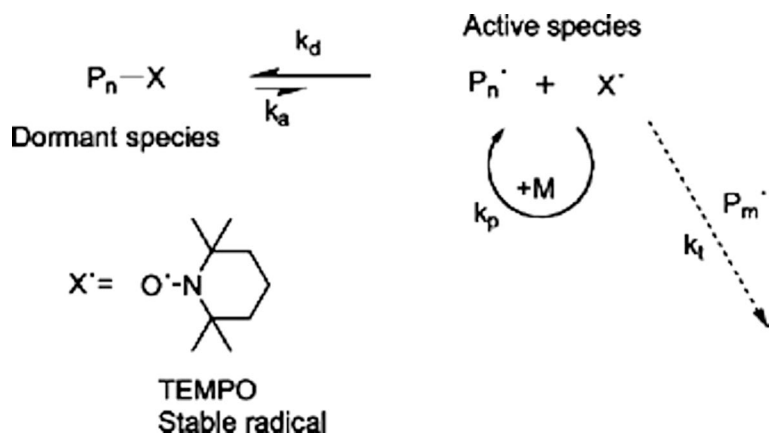

Fig. 7 Mechanism of the NMP polymerization. P_n● is the propagating chain. It may react with a monomer (M) or be terminated by reacting with a stable TEMPO radical (X●). If the propagating chain reacts with X ●, polymerization stops. Reprinted (adapted) with permission from J. Am. Chem. Soc. 2001, 123, 39, 9724–9725. Copyright 2021 American Chemical Society

be used with a wider range of monomers (Charleux et al. 2005; Nicolas et al. 2006, 2010).

NMP can be initiated by bimolecular and unimolecular initiators. Bimolecular initiation requires the presence of a typical free radical initiator and a nitroxide, such as TEMPO. Unimolecular initiation on the other hand, only requires an alkylated nitroxide or an alkoxyamine which splits into a nitroxide and an initiating species upon a temperature increase. This provides better control over the ratio of nitroxide radicals and initiating radicals. NMP with TEMPO is usually performed at high temperatures (125–145 °C), requires long reaction times (1–3 days), and is limited to styrene and 4-vinylpyridine. The use of sterically hindered nitroxides resulted in shorter reaction times, lower temperature requirements, and the ability to polymerize a wider range of monomers with low polydispersity up to molecular weights of 150,000–200,000 g/mol. Monomers that can be polymerized by NMP include styrenic monomers, vinylpyridines, acrylic esters, acrylonitrile and acrylic acid, acrylamide, *N*-substituted and *N,N*-disubstituted (meth)acrylamides, dienes, methacrylic esters, and cyclic ketene acetals. One of the drawbacks of NMP is the range of monomers that can be polymerized. The polymerization of vinyl chloride and vinyl esters such as vinyl acetate and vinyl amides is still not possible, but methacrylates can be polymerized in the presence of a comonomer. Most NMP initiators must be synthesized, but some like SG1 are already commercially available. ATRP and RAFT present advantages regarding the range of monomers that can be polymerized and the requirement of lower reaction temperatures, but NMP is a simple method that does not require post-polymerization purification other than removal of the unreacted monomer. In addition, the reaction can be started and stopped by simply increasing the temperature and cooling down (Sciannamea et al. 2008; Nicolas et al. 2013).

CNCs were modified with a derivative of SG1, (*N*-(2-methylpropyl)*N*-(1-diethylphosphono-2,2-imethylpropyl)-O-(2-carboxylprop-2-yl) hydroxylamine (commercial name BlocBuilder MA, BB) and used as macroinitiators to graft a series of monomers containing tertiary amine functionalities: DMAEMA, 2-(diethylamino)ethyl methacrylate (DEAEMA), and N-[3-(dimethylamino)propyl]methacrylamide (DMAPMAm) (Garcia-Valdez et al. 2017). These monomers polymerize into stimuli-responsive polymers which are sensitive to CO_2, providing the CNCs with increased hydrophobicity in the absence of CO_2. Grafting of the three monomers was successful, with overall polymer contents between 36 and 65 wt%.

Polystyrene was grafted from cellulose acetate as shown in Fig. 8 (Moreira et al. 2015). The synthetic route involved several steps including the functionalization of unreacted hydroxyl groups of cellulose acetate with an alkene, grafting of the BB onto the alkene functionality, and polymerization of styrene. Molecular weights above 15,000–25,000 g/mol were achieved with a polydispersity index (PDI) below 1.5 and a styrene conversion of 30%.

ATRP

ATRP is the most used polymerization technique based on transition metals applied for grafting from cellulosic materials. In ATRP, the reaction is initiated by an alkyl halide that undergoes a reversible redox reaction catalyzed by a metal complex (typically Cu), resulting in the formation of an active radical and a metal halide. The radicals can either react with monomers or with the halide in the metal complex, leaving the growing chains in a dormant state (Fig. 9) (Roy et al. 2009). One of the main challenges of using ATRP is the removal of the copper catalyst, which gives a blue/green color to the samples. Often, activators (re)generated by electron transfer (A(R)GET) ATRP is preferred due to the much lower catalyst amount required for the polymerization to occur (Kedzior et al. 2019).

ATRP can be used to polymerize a broad range of monomers, such as (meth)acrylates, (meth)acrylamides, acrylonitrile, styrenes, 1,3-dienes, 4-vinyl pyridine, 2-hydroxy ethyl(meth)acrylate, glycidyl (meth)acrylate, dimethylaminoethyl methacrylate, as well as functional monomers and macromonomers. The direct polymerization of acidic monomers using ATRP is challenging due to protonation of the ligands and intramolecular cyclization, but poly(methacrylic acid) has been successfully polymerized using variations of the ATRP technique. However, the polymerization of vinyl acetate, vinyl chloride, N-vinylformamide, N-vinylpyrrolidone and ethylene is still challenging. Most ATRP reactions are performed at temperatures between 60–120 °C, and, like NMP, can yield polymers with well-defined molecular weights up to 150,000–200,000 g/mol (Odian 2004; Lorandi and Matyjaszewski 2020). The main advantages of

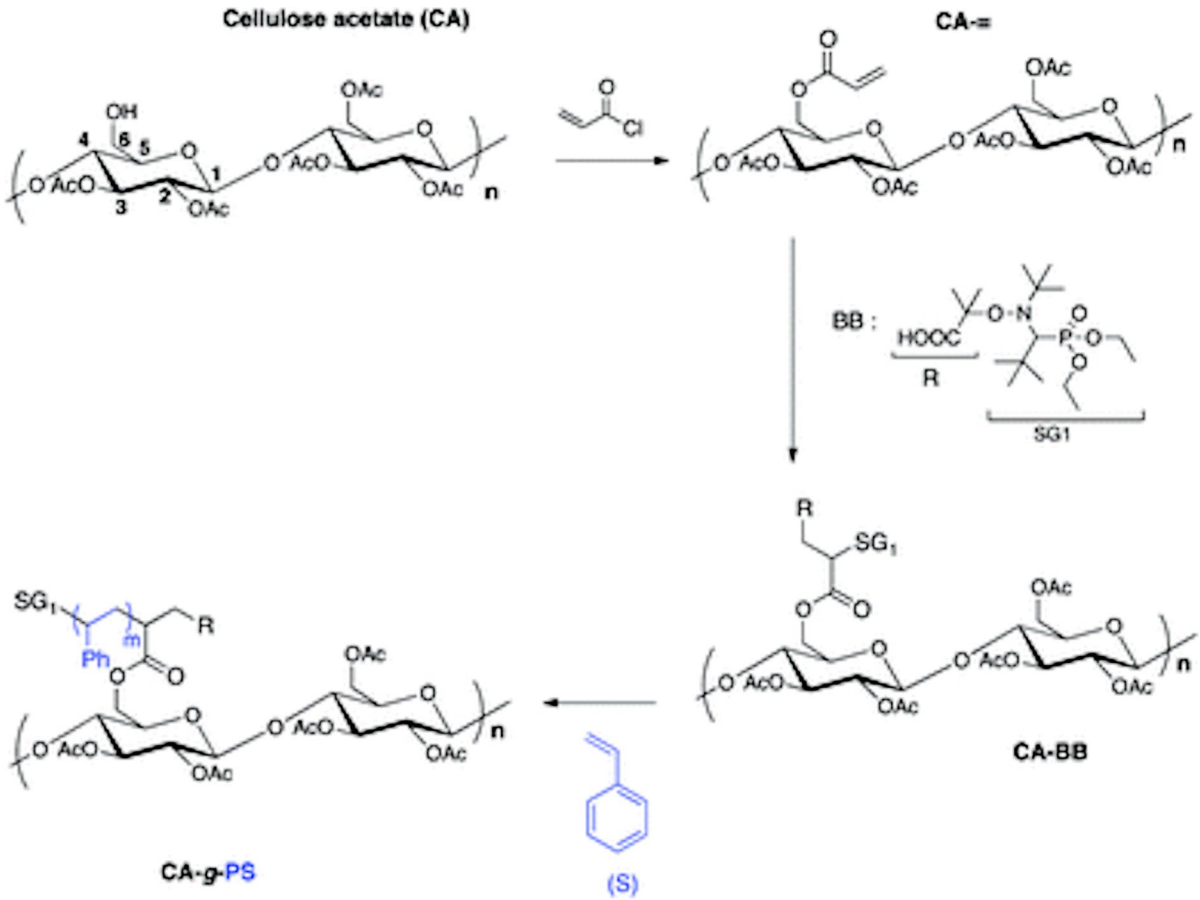

Fig. 8 Synthesis of PS- grafted cellulose acetate. Image obtained from Moreira et al. (2015)

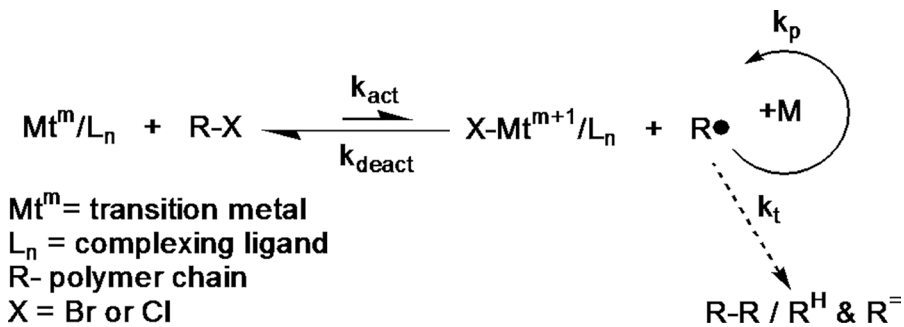

Fig. 9 Mechanism of ATRP (Matyjaszewski 2021). A halide (X) terminated polymer chain (R) reacts with Mt^m/L_n metal-ligand complex, creating R●, a radical that may grow by addition of monomer M. $X\text{-}Mt^{m+1}/L_n$ may react with the growing R●, terminating the reaction. Mt is a metal that changes oxidation state

ATRP over NMP and RAFT are that the reagents (ligands, transition metals and alkyl halides) are commercially available and that there is a vast range of alkyl halides that can be used as ATRP initiators, as for example compounds with halogen atoms activated by α-carbonyl, phenyl, vinyl or cyano groups.

The equilibrium between the dormant and the active species can be tuned by the choice of ligand. Another advantage of ATRP is that it can tolerate the presence of oxygen and other inhibitors. One of the main challenges of using ATRP is the removal of the copper catalyst, which gives a blue/green color to the samples and can be mildly toxic. Often, activators (re) generated by electron transfer (A(R)GET) ATRP is preferred due to the much lower catalyst amount required for the polymerization to occur (Braunecker and Matyjaszewski 2007; Kedzior et al. 2019).

CNCs from cotton wool were grafted with styrene. The surface of the CNCs was first modified with 2-bromoisobutyryl bromide (BiB) to introduce reaction sites for ATRP, and then styrene was grafted from the active sites (Morandi et al. 2009). A sacrificial initiator was used to obtain higher control on the degree of polymerization of the grafted chains. By varying the ratio between monomer and sacrificial initiator, degrees of polymerization between 27 and 171 were obtained, equivalent to 8–22 wt% of grafted polystyrene. The contact angle of the CNCs increased from 43 to 94°. The hydrophobic properties of the modified CNCs were advantageous for their use as absorbents of organic pollutants from water. Grafting of 68% styrene on CNCs with a molecular weight (M_n) of 74,700 g/mol and a PDI of 1.21 has been achieved using the same initiator (Yi et al. 2008).

Filter paper was modified at the surface with methyl acrylate using BiB (Carlmark and Malmström 2002). Grafted polymers with degrees of polymerization of 149 and 298 were obtained, and the modified surfaces presented advancing contact angles of 128° and 133°, respectively. ARGET ATRP was used to graft MMA, styrene and GMA from filter paper (Hansson et al. 2009). Molecular weights in the range of 8100–30,100 g/mol were obtained for PMMA, 6200–24,800 g/mol for PS, and 10,600–17,600 g/mol for PGMA. The contact angles for PMMA-grafted substrates were 109°–112°, while for PS-grafted substrates they were 132°–135°. In the case of paper modified with PGMA, the surfaces remained hydrophilic when washed with protic solvents. The use of aprotic solvents maintained the epoxide groups on the surface, increasing the stability of deposited water droplets. The same technique was used to graft poly(lauryl acrylate) and poly(octadecyl acrylate) with molecular weights (M_n) up to 7300 and 6800 g/mol and contact angles of up to 135° and 146°, respectively (Arteta et al. 2017). The modified filter papers showed an increased ability to remove hydrophobic pollutants compared with unmodified filter paper.

The surface of wood was also grafted using the ARGET ATRP technique (Fu et al. 2012). PMMA was grafted with grafting yields between 2.4 and 12.8%. Hydrophobic surfaces were obtained with contact angles in the range of 74°–130°. Similarly, the surface of filter paper was grafted with GMA using BiB as initiator. After ring-opening of GMA, the hydroxyl end-groups were further modified with pentadecafluorooctanoyl chloride to increase the hydrophobicity of the substrate. A contact angle of 154° was obtained after fluorination (Nyström et al. 2006). To obtain higher hydrophobicity of the surface, a "graft-on-graft" approach was used. The hydroxyl end-groups of the grafted PGMA were modified with the initiator, and another polymerization reaction was performed and followed by fluorination of the end-groups, as shown in Fig. 10. The thus modified paper displayed a contact angle of 172°. The same strategy was used on cotton fabric, grafting first GMA and then heptafluorobutyryl chloride (Li et al. 2015). Contact angles between 140–155° were obtained by increasing the concentration of fluoroalkyl compound. Since the hydrophobicity of the surface was not stable over time, a "graft on graft" approach and subsequent fluorination were performed, increasing the contact angle to 163.7°, and providing a stable superhydrophobic coating.

Spruce wood samples were grafted with the hydrophobic polymer PTFEMA via surface initiated AGET-ATRP (Vidiella del Blanco et al. 2019). A macroinitiator for ATRP was prepared by grafting BiB. Some samples were swollen in dichloromethane to limit the modification to the lumen/cell wall interface, while other samples were swollen in pyridine to allow to graft BiB deep inside the cell walls. The same grafting percentage was obtained with both types of macroinitiators (ca. 43%), and it was shown that the polymerization of TFEMA occurs at the surface of the wood samples up to a few hundred microns in depth regardless of the pre-conditioning of the samples.

BiB was immobilized onto filter paper, which was used as a substrate for grafting of the thermoresponsive monomer *N*-isopropylacrylamide (NIPAAm) (Lindqvist et al. 2008). The polymer

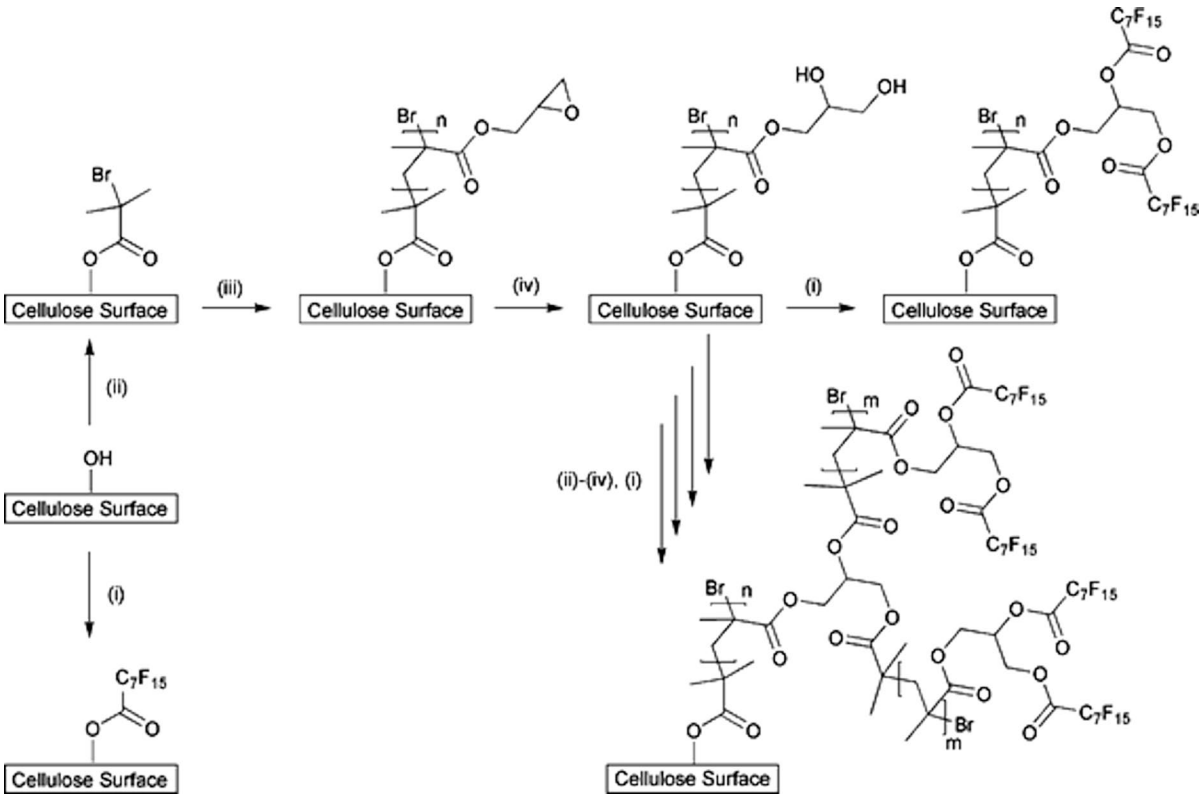

Fig. 10 Synthetic route of the modification of cellulose. Reaction conditions: (i) pentadecafluorooctanoyl chloride, triethylamine (TEA), 4-dimethylaminopyridine (DMAP), dichloromethane, room temperature (RT); (ii) 2-bromoisobutyryl bromide, TEA, DMAP, THF, RT; (iii) GMA, CuCl, $CuBr_2$, N,N,N',N'',N''-pentamethyldiethylenetriamine (PMDETA), toluene, 30 °C; (iv) HCl(aq), THF, RT. Image obtained from Nyström et al. (2006)

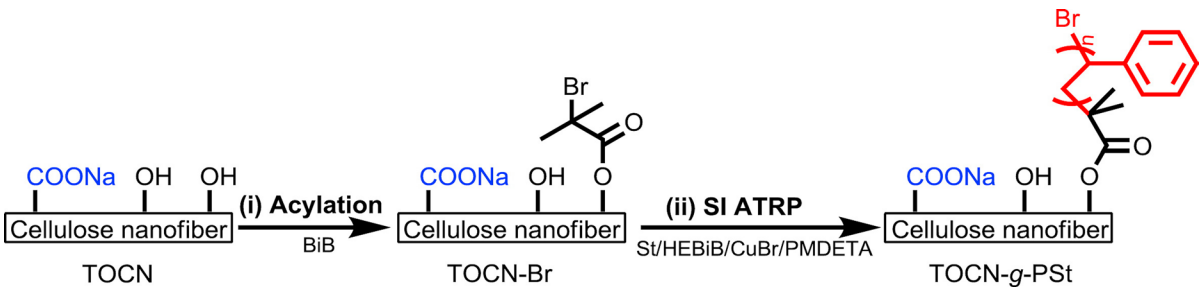

Fig. 11 Reaction scheme of the synthesis of PS-grafted TOCNFs (TOCN) via ATRP. Image obtained from Huang et al. (2015)

poly(N-isopropylacrylamide) (PNIPAAm) is hydrophobic above ~32 °C. The grafted paper presented a contact angle of 110° at 50 °C. A "graft-on graft" polymerization was performed, where PGMA was used as the first grafted polymer. The surface with the new PGMA-g-PNIPAAm coating displayed a contact angle of 130°. Similarly, P4VP, a pH-responsive polymer, was grafted from filter paper. The surfaces achieved contact angles of 90°–100° at pH 7 and of 125° at pH 9. The grafting of first PNIPAAm and then P4VP resulted in surfaces that were both pH- and temperature-responsive and that reached contact angles up to 120° at 50 °C and pH 9.

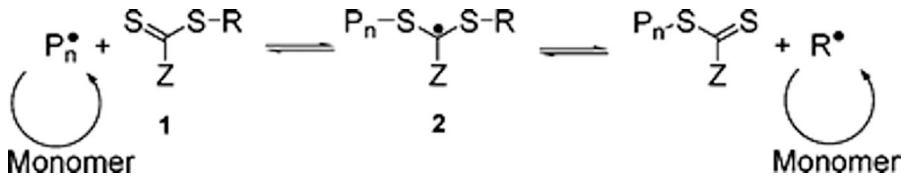

Fig. 12 Mechanism of RAFT polymerization. Image obtained from Roy et al. (2009) A polymer radical chain $P_n^{\bullet}$, may react with a monomer. The reaction is paused by reversibly binding with a labile thiocarbonyl moiety

TEMPO-oxidized CNFs (TOCNFs) were grafted with styrene via surface-initiated ATRP (SI-ATRP) as depicted in Fig. 11 (Huang et al. 2015). Carboxylic acids in TOCNFs deactivate the copper catalyst, preventing the polymerization reaction from occurring. By preparing the acid salt of the TOCNFs, the carboxylic groups are neutralized, and it is possible to conduct ATRP. BiB was first grafted onto the surface of the TOCNFs and then the polymerization of styrene took place. Polystyrene molecular weights between 14,100 and 29,000 g/mol were obtained and the contact angles of dry grafted TOCNFs were between 85.1 and 98.7°. The modified CNFs are promising materials for the absorption of organic pollutants.

Bacterial nanocellulose membranes were grafted with MMA and BA (Lacerda et al. 2013). The surface of the membranes was first modified with BiB and then with either MMA, BA, or MMA-co-BA. The molecular weight of BNC-PMMA was 2.7×10^5 Da, and that of BNC- PMMA-*co*-PBA was 3.7×10^5 Da. Grafting of PMMA and PBA increased the hydrophobicity of BNC, with contact angle values of 134° for BNC-PMMA and 116° for BNC-PBA.

RAFT

Unlike ATRP and NMP that are based on reversible termination mechanisms, RAFT is based on reversible chain transfer. RAFT polymerizations are performed in similar conditions than radical polymerizations, but they require the presence of a chain-transfer agent (RAFT agent). These RAFT agents reversibly transfer a labile end group (typically dithiocarbamates, dithiocarbonates, or dithioesters) to a propagating chain. The labile end-group is reversibly exchanged between different growing polymer chains. The raft agents also contain R and Z groups which allow tuning the reaction kinetics and equilibrium between the dormant and active states (Fig. 12). The architecture of the RAFT agents is determined by the reaction conditions and the choice of monomers. The main challenges of RAFT polymerizations are that RAFT agents are not commercially available and that the resulting polymers have inherent colors and odors caused by the dithioester groups. However, these groups can be easily cleaved (Odian 2004; Moad et al. 2005).

Among the controlled radical polymerization methods, RAFT allows the polymerization of the widest range of monomers, which include (meth) acrylates, (meth)acrylamides, and styrenic monomers, and vinyl monomers. The polymerization is performed in the same solvents as free radical polymerizations, including protic solvents such as water and alcohols, and using the same initiators and temperature range, which can vary from ambient temperature to 140 °C (Odian 2004; Moad et al. 2005). Nevertheless, there are few examples of polymer grafting from cellulosic materials using RAFT. In most cases, hydrophobic polymers such as PS, poly(methyl acrylate) (PMA) and PMMA have been grafted from cellulosic materials. However, in many of these examples the contact angle of the samples was not measured.

PMMA/CNC composites were prepared using two different methodologies based on RAFT polymerization (Anžlovar et al. 2016). First, the CNCs were modified with a RAFT chain transfer agent and then two different pathways were followed: i) in-situ grafting of MMA during bulk polymerization of the PMMA/CNC composite, and ii) grafting of MMA from the CNCs followed by dispersion of the CNCs and bulk polymerization of MMA. The reaction scheme of MMA grafting from CNCs is shown in Fig. 13. Both approaches resulted in composites with improved tensile strength (11 and 10%, respectively), Young's modulus (24 and 10%), and Charpy impact resistance (11 and 7%) compared with pure PMMA. Composites prepared with unmodified CNCs

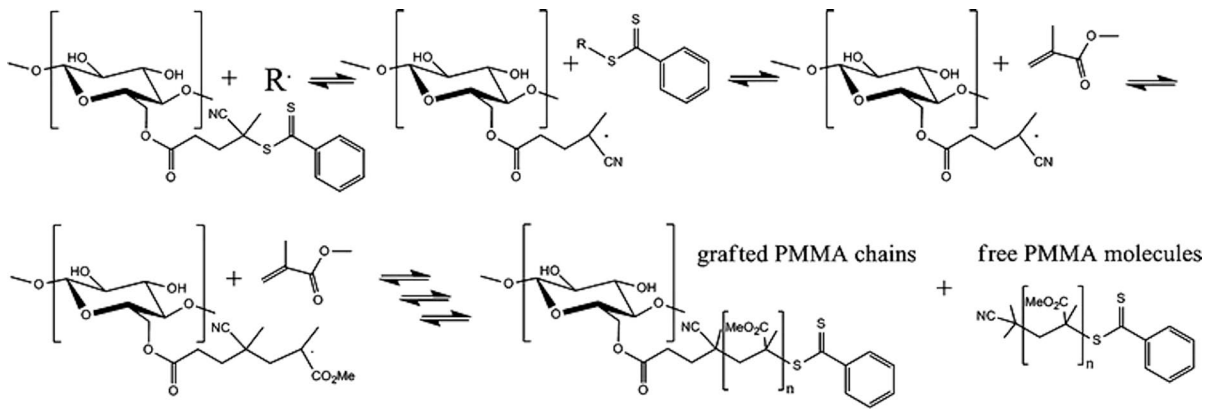

Fig. 13 Grafting of MMA from CNCs via RAFT polymerization. Image obtained from Anžlovar et al. (2016)

presented a decrease in the mechanical properties due to aggregation of the CNCs.

Grafting of PVAc from CNCs was performed by RAFT and macromolecular design via the interchange of xanthates (MADIX, RAFT/MADIX) polymerization using two different grafting procedures (Boujemaoui et al. 2016). DPs of 57 and 230 were targeted, resulting in molecular weights of 3630 and 3880 g/mol for DP = 57, and 15,930 and 16,270 g/mol for DP = 230. Nanocomposites of PVAc with grafted CNCs were prepared and they presented improved mechanical properties than composites with unmodified CNCs, achieving up to 154% higher Young's modulus.

Hydroxypropyl cellulose and methyl cellulose were modified by RAFT polymerization (Fleet et al. 2008). Grafting of VAc from the active sites resulted in the formation of an amphiphilic copolymer. After grafting the molecular weights of hydroxypropyl cellulose and methyl cellulose increased from 64,000 and 32,000 g/mol to 450,000 and 600,000 g/mol, respectively. PVAc, poly(butyl acrylate), PS and cationic amphiphilic PS/poly(4-vinylbenzyl chloride) (PS-PVBC) copolymers were grafted from wood fibers (Tastet et al. 2011). Grafted polymers with a wide range of molecular weights (600–33,700 g/mol) were obtained. Contact angles between 90° and 95° were obtained for fibers coated with PS and PS-PVBC. Additional experiments showed that wood pellets prepared with blends of crude fibers and PS-grafted fibers were only hydrophobic when all the fibers were grafted. On the other hand, hydrophobicity could also be achieved when the pellets were coated with grafted fibers amounting to 9% of the total weight.

Styrene, MA and MMA were grafted from the surface of cotton fabric, which previously had been modified with a RAFT chain transfer agent (Perrier et al. 2004). The polymerizations reached full conversion of the monomers and the molecular weights were 106,900 g/mol for styrene, 84,850 g/mol for MA, and 60,500 for MMA. Hydrophobic filter paper was prepared by grafting styrene (Roy et al. 2005). Prior to polymerization, the paper was modified with a chain transfer agent, as shown in Fig. 14. The water contact angles were around 130°, and the grafting ratio was comparable to that obtained by ATRP under similar conditions. The initial contact angle on unmodified filter paper was impossible to determine, due to quick sorption of water.

In-situ polymerization

A one-pot synthesis was used to prepare waterborne polyurethane (WPU)/CNC composites. The grafting reaction occurred by first modifying polycaprolactone diol with isophorone diisocyanate, and then adding the CNCs to the reaction mixture (Cao et al. 2009). The reaction between the hydroxyl groups on the CNCs and the isocyanate functionality resulted in the formation of polyurethanes. Grafting densities of 45.7–57 wts% were obtained with this method, and the WPU/CNC composites presented improved mechanical and thermal properties.

Grafting of poly(ionic liquid)s (PILs) has also been suggested as a method to obtain hydrophobic CNFs

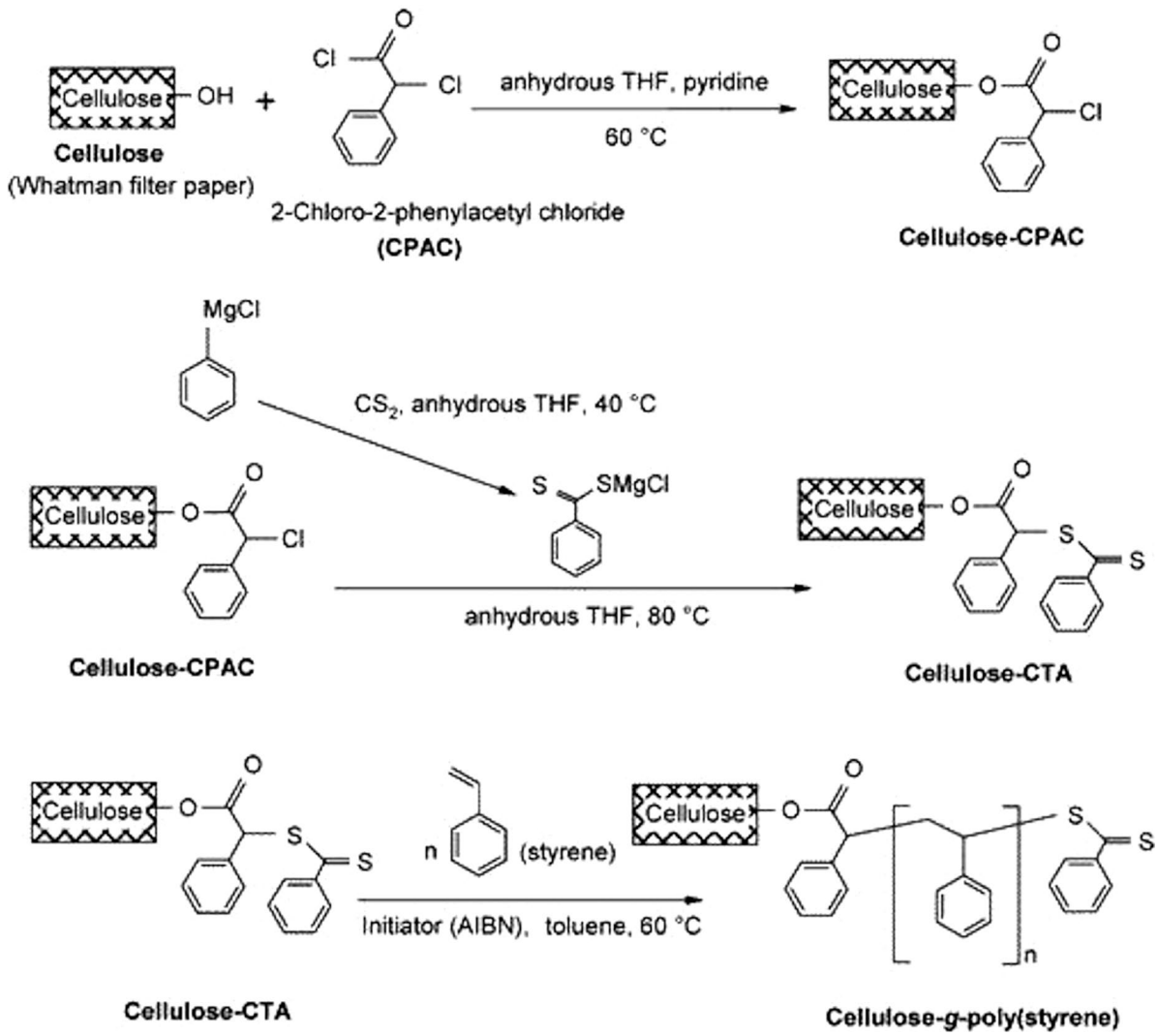

Fig. 14 Synthesis of Cellulose RAFT chain transfer agent followed by polymerization of styrene. Reprinted (adapted) with permission from Macromolecules 2005, 38, 25, 10363–10372. Copyright 2021 American Chemical Society

(Grygiel et al. 2014). PILs were electrostatically grafted onto TOCNFs by in situ polymerization of 1-ethyl-3-vinylimidazolium bromide (PIL-Br) without requiring any functionalization of the TOCNFs. The thermal stability of the CNFs was maintained after grafting, and the possibility of exchanging the anions present in the PILs allows the dispersibility of the modified CNFs in a wide range of solvents. Hydrophobic CNFs were obtained by replacing the bromide anion with bis(trifluoromethylsulfonyl)imide (TF_2N), which were soluble in dimethyl sulfoxide (DMSO), and with hexafluorophosphate, which were soluble in DMSO, acetone and methanol. The modified CNFs were used as reinforcements for PIL membranes, presenting higher Young's modulus and stress at failure than non-reinforced membranes (Fig. 15). Table 4 shows the two in-situ polymerization methods described in this section.

Radiation-induced modifications

Grafting of cellulosic materials can also be initiated using radiation sources such as ultraviolet light, gamma radiation, and plasma. These techniques

Table 4 Overview of modifications of cellulosic materials by in-situ polymerization

Source of cellulose	Type of cellulose	Monomer	Grafting yield (%)	References
Cotton linter	CNC	Polycaprolactone diol	45.7–57	(Cao et al. 2009)
Softwood pulp	CNF	PIL-TF_2N/PF_6	70	(Grygiel et al. 2014)

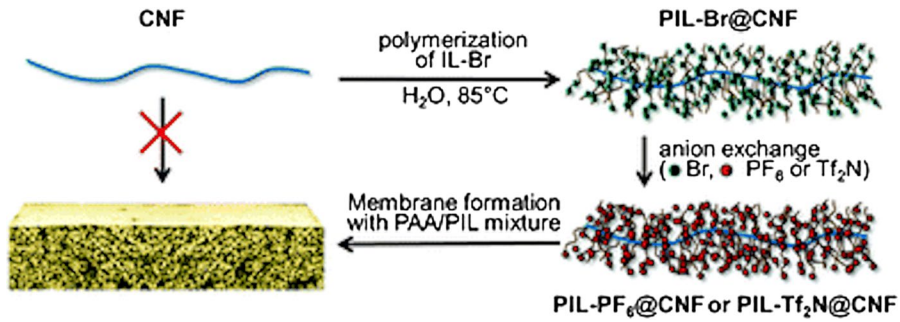

Fig. 15 Synthesis of CNF-reinforced porous PIL membrane via one-step surface grafting. Image obtained from Grygiel et al. (2014)

generate radicals that can be used as initiators for graft polymerizations. Radiation-induced modifications are a "grafting from" technique, and as previously described in the *free raadical polymerization* section, polymerization occurs via the free radical polymerization mechanism. However, to improve the readability of this review, radiation-induced modifications are described in a separate section. Table 5 shows a summary of all the references discussed in this section of the review.

UV initiated polymerization

The synthesis of polymers using ultraviolet (UV) radiation is possible when photoinitiators are present. The irradiation of these initiators with UV light generates radicals that can start polymerization reactions. The advantages of using UV polymerization are the simplicity of the method, the absence of organic solvents, the high degree of grafting, and the lack of homopolymer formation. Some examples of polymer grafting by UV light are listed below.

Glycidyl methacrylate was grafted from cotton fibers using both photoinitiators and chemical initiators (Shukla and Athalye 1994). Uranyl nitrate, CAN and benzoin ethyl ether were chosen as photoinitiators, and CAN and KPS as chemical initiators. The optimal reaction conditions were found for each initiator, resulting in grafting yields between 8.95 and 26.20%. Slightly higher grafting was obtained when CAN was used as photoinitiator (26.20%) instead of chemical initiator (24.13%). The same photoinitiators were used to graft styrene from cotton fibers (Shukla et al. 1993). Uranyl nitrate was the initiator that provided the highest grafting yields, reaching 1.10%. Both in the grafting of GMA and styrene, preswelling the fibers resulted in higher grafting due to the opening of the fiber structure.

The photo-sensitizer 2-ethylanthraquinone was used to graft polymers from cotton fabric via light-induced surface radical polymerization (Zhuo and Sun 2014). The proposed reaction mechanism is shown in Fig. 16. 2-ethylanthraquinone generates radicals and active oxygen species when exposed to UV or day light. After dyeing the fabrics with the photosensitizer, the grafting of the hydrophobic monomers butyl acrylate, 1*H*, 1*H*, 5*H*-octafluoropentyl acrylate (OFA), and styrene was attempted, as well as grafting of two hydrophilic monomers (acrylamide and [2-(methacryloyloxy) ethyl] dimethyl-(3-sulfopropyl) ammonium hydroxide). All monomers were successfully grafted except for styrene, which quenches the photoinitiator. The modified fabrics displayed remarkable antibacterial properties.

Hydrophobic filter paper was obtained by grafting perfluoropolyether urethane methacrylate (Bongiovanni et al. 2011). Benzophenone was used as photoinitiator. The grafted papers presented large water contact angles (120–140°), depending on the reaction conditions, as well as lipophobic properties and excellent resistance to grease and oil.

Table 5 Overview of modifications of cellulosic materials by radiation-induced polymerization

UV

Cellulose source	Type of cellulose	Monomer	Grafting yield (%)	Grafting efficiency (%)	Contact angle (°)	References
Scoured, bleached cotton yarn	Fibers	GMA	~8.95–26.20%			(Shukla and Athalye 1994)
		Styrene	0–1.10			(Shukla et al. 1993)
Bleached, desized cotton fabric	Fibers	BA, OFA, styrene	Styrene: 0%			(Zhuo and Sun 2014)
Whatman filter paper	Fibers	Perfluoropolyether urethane methacrylate			120–140	(Bongiovanni et al. 2011)
Whatman filter paper	Fibers	MMA				(Garnett et al. 1999)
Whatman filter paper	Fibers	MMA	0.36–89	77–88		(Margutti et al. 2002)
		Ethylacrylate	14			
		MA	28			
Wood pulp	CNC	MMA	477.2	79.7		(Wang et al. 2016)
		BA	311.2	75.4		
		NIPAAm	292.4	73.5		
Japanese cypress wood powder	CNF	MMA	8–484		91.3, 99.7	(Yang et al. 2019)
		Butyl methacrylate	131		113.4	
		BA	88		119.7	
		HEMA	59		75.7	
		Acrylonitrile	210		64.3	
		MMA-co-styrene	41		116.5	

Gamma radiation

Cellulose source	Type of cellulose	Monomer	Grafting yield (%)	Contact angle (°)	References
Cotton-cellulose bleached woven fabric	Fibers	GMA	PIG < 111 SG < 350		(Desmet et al. 2011)
	MCC	GMA			(Madrid and Abad 2015)
Whatman filter paper	Fibers	Styrene	< 55	123–138	(Barsbay et al. 2007)
Jute fibers	Fibers	MMA	< 73%		(Khan 2005)
Cotton fabric	Fibers	DEAETPN, MMA	0–32		(Verma and Kaur 2012)
	Methyl-cellulose, CNC	TMPTMA			(Sharmin et al. 2012)

Plasma polyerization

Cellulose source	Type of cellulose	Monomer	Contact angle (°)	References
Cotton fabric	Fibers	Styrene	91–133	(Parida et al. 2012)
Cotton fabric	Fibers	HMDSO	< 162	(Yang et al. 2018)
Viscose rayon	Fibers	1,3-Butadiene	< 90–143	(Samanta et al. 2012)
Ramie fibers	Fibers	Propylene	96–106	(Zhang et al. 2015)
		Propane	97.6	

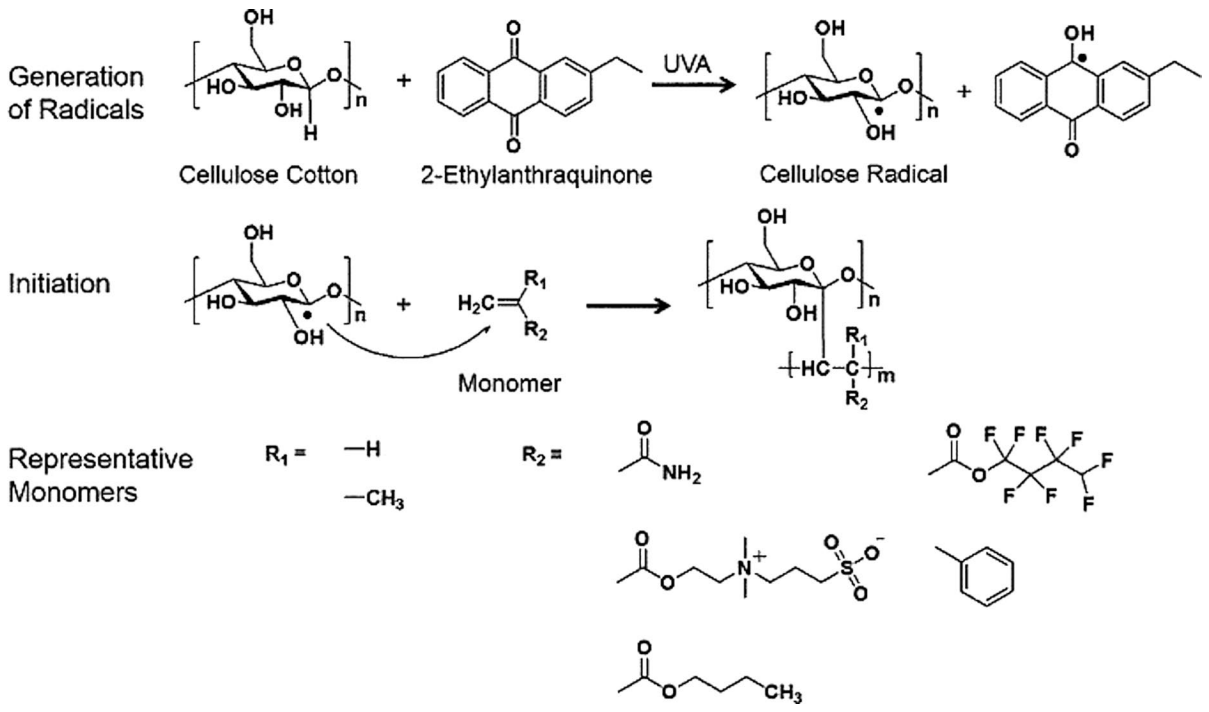

Fig. 16 Suggested mechanism for light-induced polymer grafting onto activated cellulose. Image obtained from Zhuo and Sun (2014)

MMA was grafted from filter paper using several photoinitiators (benzoin ethyl ether, Irgacure 184, 1700, 1800, and Darocure 1173) (Garnett et al. 1999). The grafting reactions were performed with UV light and ionizing radiation. The effect on the grafting of monomer concentration, acid pH, nitrogen atmosphere, presence of styrene comonomer, addition of vinyl ether additives and charge transfer monomers was investigated, resulting in a wide range of grafting percentages. The use of charge transfer monomers allows the synthesis of copolymers using a one-step method.

Wang et al. (2016) immobilized the photoinitiator bis(acyl)phosphane oxide at the surface of CNCs and grafted MMA, BA, NIPAAm, and 2-hydroxyethyl acrylate. The highest grafting yield was obtained for the polymerization of MMA, and the lowest for the polymerization of the hydrophilic monomer 2-hydroxyethyl acrylate. CNCs grafted with PMMA were incorporated into a PMMA matrix as reinforcement. The grafted CNCs increased the elastic modulus of PMMA by 8% while maintaining the tensile strength constant.

CNFs were grafted with MMA by irradiating the microfibrils with UV light (Yang et al. 2019). Radicals were generated at the surface of the CNFs in aqueous media without the need for an initiator or organic solvents. Grafting increased the hydrophobicity of the CNFs and enabled their dispersion in organic solvents. The grafted PMMA had molecular weights in the range of 640–1330 kg/mol. Films were prepared by hot pressing from two samples of grafted CNFs with different degrees of grafting and displayed contact angles of 91.3 and 99.7°. TOCNFs and CNCs were grafted with PMMA following the same procedure, where TOCNFs achieved the highest grafting degree and CNCs the lowest, compared with CNFs. Grafting of CNFs was also successfully performed with n-butyl methacrylate, 2-hydroxyethyl methacrylate (HEMA), BA, *N,N*-dimethyl acrylamide, and acrylonitrile. Except for poly(*N,N*-dimethyl acrylamide), all grafted polymers increased the hydrophobicity of the CNFs, including the hydrophilic polymer PHEMA. However, the water contact angles of CNFs grafted with polyacrylonitrile and PHEMA were below 90°.

Grafting of methyl methacrylate was performed on previously oxidized cellulose, which contained dialdehydic groups where the monomers were grafted

(Margutti et al. 2002). The polymerization occurred using vaporized acrylic monomers. The increase in the oxidation of the cellulose led to a higher grafting percentage. Additional samples were prepared by grafting MMA, ethylacrylate and methyl acrylate from oxidized cellulose that had been irradiated with UV light prior to the polymerization. Pre-irradiation of oxidized cellulose results in the activation of the aldehyde groups. Pre-irradiated samples that were polymerized with MMA for 1 h achieved a similar grafting percentage as samples that were polymerized during 5 h without pre-irradiation. In addition to decreasing the grafting time, pre-irradiation also enhances the penetration of the monomer within the fibers and results in a lower formation of homopolymer (7–15%).

Gamma Radiation initiated polymerization

Gamma radiation is a high energy ionizing radiation that leads to the formation of ions and radicals, which in turn can polymerize vinyl and acrylic monomers. There are two different approaches used in polymerization reactions with gamma rays: pre-irradiation grafting (PIG) and simultaneous grafting (SG). Gamma irradiation is typically used for grafting of textiles. In the PIG technique, the fabric is first irradiated and then immersed in a monomer solution, whereas in the SG technique, the fabric is irradiated while immersed in the monomer solution.

In one example, the hydrophobicity of cotton fabric was increased by grafting GMA with gamma radiation using the PIG and SG techniques (Desmet et al. 2011). Simultaneous grafting resulted in higher efficiencies (55% for PIG and 350% for SG under the same conditions). However, SG leads to the formation of homopolymers not grafted to the substrate caused by radicals generated in the solvent. The modified fabric presented reduced water sorption. At higher degrees of grafting, the SG samples were more hydrophobic than the PIG ones because SG occurs on the surface, while PIG occurs through the cross-section of the fabric. Modification of the cellulose samples with GMA increased their ability to adsorb aromatic pollutants from water. Similarly, GMA was grafted onto microcrystalline cellulose (MCC) by simultaneous grafting (Madrid and Abad 2015). The highest grafting was achieved in mixtures of methanol/water solutions, although large amounts of homopolymer were obtained. Further grafting experiments performed in methanol resulted in degrees of grafting up to 20%.

Barsbay et al. (2007) grafted styrene from filter paper via RAFT polymerization initiated by gamma radiation as illustrated in Fig. 17. A grafting degree of 55% was achieved when the reaction was performed in methanol, and up to 39% when it was performed in a dioxane/water mixture. The contact angles of samples with 20, 30 and 39% grafting were 123, 134, and 138°, respectively. The grafted chains were cleaved from the substrate and characterized by SEC, presenting molecular weights between 6500 and 14,500 g/mol and PDIs in the range of 1.13–1.18.

Another example of polymer grafting by gamma radiation is the modification of jute fibers with PMMA (Khan 2005). Pre-irradiated fibers were immersed in an MMA solution. The radicals can be formed by hydrogen and hydroxyl abstraction or C–C and C-O bond cleavage in the cellulose, hemicellulose and lignin molecules. Additionally, lignin can

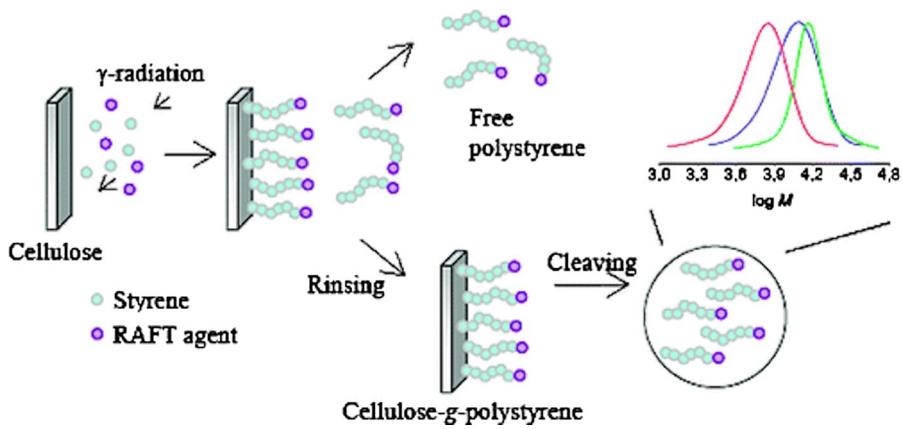

Fig. 17 Schematic representation of cellulose grafting with gamma radiation. Reprinted (adapted) with permission from Macromolecules 2007, 40, 20, 7140–7147. Copyright 2021 American Chemical Society

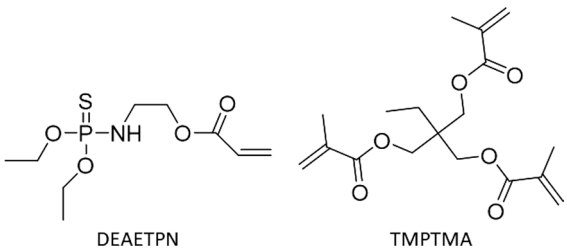

Fig. 18 Chemical structure of DEAETPN and TMPTMA

act as a reaction inhibitor. Fibers pre-irradiated in air achieved higher grafting percentages (73%) than fibers pre-irradiated in nitrogen atmosphere (53%). The effect of temperature and monomer concentration were also investigated, showing that increasing temperature and monomer concentration resulted in higher grafting percentages.

Gamma radiation has also been used for grafting of more uncommon monomers such as diethyl (acryloyloxy) ethylthiophosphoramidate (DEAETPN) and trimethylolpropane trimethacrylate (TMPTMA) (Fig. 18). DEAETPN was synthesized and grafted from cotton fabric to provide flame retardant properties. Copolymerization with small amounts of MMA improved the grafting efficiency of DEARPN (Verma and Kaur 2012). The hydrophobic monomer TMPTMA was used in methylcellulose films in presence of glycerol to improve the mechanical properties and decrease the water vapor permeability of the films (Sharmin et al. 2012). The addition of CNCs to these films contributed even further to the decrease in the water vapor permeability, due to the increasing tortuosity of the films.

Plasma

The general mechanism of plasma grafting occurs via three steps: i) activation of the surface, ii) formation of peroxide radicals, and iii) polymerization, as illustrated in Fig. 19. In the first step, hydrogen is extracted from the cellulose chains, leading to the appearance of radicals. These radicals react with oxygen, forming peroxides, which can further decompose into new radical species and start a polymerization reaction when they are in the presence of a monomer (Couturaud et al. 2015).

There are many examples of preparation of hydrophobic textiles using plasma. Grafting hydrophobic molecules can result in both covalently attached polymer chains and also deposition of polymers onto the surface of the fabric. Grafted and deposited polymers contribute to increasing the hydrophobicity of the substrate, however, only the covalently attached polymers will remain after washing the textiles. Therefore, it is important to characterize the fabrics after washing to assess whether hydrophobicity is attained. Examples of modified textiles are given below.

Styrene/helium plasma was used as a method to obtain hydrophobic cotton fabric samples with contact angles between 107° and 133° (Parida et al. 2012). After washing the samples, the water contact angles decreased slightly (about 20°) due to the removal of polystyrene deposited at the surface but remained hydrophobic. Raman spectroscopy characterization suggested that the hydrophobicity of the fabric is caused by grafting of styrene and benzene radicals to the cellulose molecules, but not the formation of polymers. A single-step graft polymerization of hexamethyldisiloxane (HMDSO) onto cotton fabric was performed in both N_2 and O_2 plasma (Yang et al. 2018). The fibers were coated by a thin layer of nanoparticles that provided the sample with hydrophobic properties. The reactions performed with O_2 plasma achieved higher contact angles (162°) than those performed with N_2 plasma (149°). The contact angles of the samples only decreased slightly after storage in ambient conditions or laundering, demonstrating the stability of the coatings. In addition,

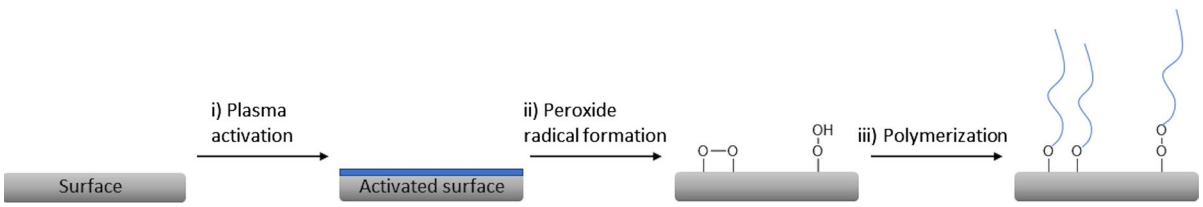

Fig. 19 The three stages of polymer grafting using plasma

the fabric appearance and air permeability were not affected by the grafted polymer.

He/1,3-butadiene plasma was used to obtain hydrophobic viscose rayon (Samanta et al. 2012). Increasing the plasma treatment time increased in the water absorbency time of the textile. Water contact angles up to 143° were achieved. After washing the tissue with soap, both the water absorbency time and the contact angles decreased. However, the washed substrates remained hydrophobic, with contact angles up to 134°. In the article, it is hypothesized that butadiene fragments and oligomers react with the cellulose molecules, whereas the polymers that are formed are only deposited at the surface and removed during washing.

Ramie fibers were modified with propylene and propane in plasma (Zhang et al. 2015). Increasing the exposure to plasma resulted in increasing roughness of the surfaces due to peeling off of the fibers, but excessive exposure led to smoothing of the surface due to the peeling off effect. Several samples were modified with propylene and presented contact angles up to 106°. A sample was prepared with propane as a comparison and a contact angle of 97.6° was obtained. In both cases, when polypropylene composites were prepared, grafting led to an increased adhesion with the polypropylene matrix.

Summary and outlook

This review presents an overview of the state-of-the-art of (nano)cellulose hydrophobization using polymers. At a first glance, polymer adsorption seems the simplest approach to modify cellulosic materials. However, some applications might require covalent bonding between the polymers and the substrates, for instance for filtration purposes, or in clothing items that must undergo several cycles of washing. Amongst all the grafting techniques, radiation-induced polymerizations typically are more environmentally friendly, even though they offer little control on the polymerization process. It is the same case for radical polymerization, where the simplicity of the polymerization reaction comes at the expense of the control on the properties of the grafted polymers. Ring opening polymerization allows grafting of biodegradable polymers such as PLA and PCL, which are two of the most environmentally friendly alternatives when it comes to synthetic polymers. Controlled radical polymerization involves more complex systems that provide well-defined polymers. This can be of interest when one wants to finely tune the substrates.

The articles cited in this review show a clear tendency over time towards more complex architectures when it comes to polymer grafting, and also towards more environmentally friendly solutions, either by the choice of reagents, experimental design, or application of the materials. Hydrophobic cellulosic materials open possibilities of new sustainable products and profit from a resource as easily available as wood. Polymer biocomposites is one of the application areas that clearly benefit from polymer grafting on cellulosic materials. The possibility of modifying the cellulosic reinforcement with the same polymer as the matrix highly increases the compatibility between the two components of the composite.

Radiation-induced modifications are the techniques with the highest potential for industrialization. For example, both the textile and packaging industry are sectors that could benefit from implementing plasma for modification of the fabric and packaging surface properties. Although the technology is available, plasma is not implemented yet for grafting purposes due to the high costs associated with it, such as the need to have expensive vacuum equipment (Cvelbar et al. 2019). Other products such as grafted CNCs and CNFs are not of industrial interest due to their high production costs. The only implementation area for grafted CNCs and CNFs could be very specialized fields where very small amounts of product are required, such as the pharmaceutical one (Kedzior et al. 2019).

The reviews Hydrophobization of lignocellulosic materials parts I, II, and III give an overview of the state-of-the-art of the different hydrophobization methods used with lignocellulosic materials. There are several general observations that can be drawn from the three reviews. In general, the physical modification methods (adsorption and plasma) seem the simplest modification approaches. Adsorption of "short" molecules typically only decreases the hydrophilicity of the substrates without creating a hydrophobic surface, while adsorption of polymers often yields highly hydrophobic surfaces. On the other hand, plasma modifications, by both etching and (polymer) grafting usually form highly hydrophobic surfaces. Regarding grafting

reactions in general, some of them such as esterification and silylation are more well established than others. These two types of reactions have the advantage that they can be performed in the gas phase or in aqueous medium, and therefore do not require the use of solvents. It is the same case for radiation-induced modifications, which do not involve the use of solvents and are also regarded as environmentally friendly technologies. Lastly, reactions such as controlled radical polymerization or click-chemistry reactions allow the functionalization of substrates with very complex structures and high control but have limited industrial applicability due to the high cost of the products.

Hydrophobization of lignocellulosic materials is a subject of great importance in the current social and political situation, where the use of single-use plastics in Europe has been banned. This is an opportunity to take the research in this field a step towards industrialization, particularly for single-use products such as packaging or cutlery and plates. Looking forward, the short-term goal should be the upscaling and economic viability of the hydrophobization processes.

Acknowledgments The authors would like to acknowledge the Research Council of Norway, and their funding of the NanoPlasma project (274975).

Authors' contributions SR-F: literature search and analysis, writing and revision of the manuscript. JT: idea for the article, literature search and analysis, writing and revision of the manuscript. LJ: idea for the article, revision of the manuscript. KS: idea for the article, revision of the manuscript.

Funding Open access funding provided by RISE Research Institutes of Sweden.We greatly acknowledge the Research Counsel of Norway, and their funding of the NanoPlasma project (274975).

Declarations

Conflict of interest All the authors declare no conflicts of interest.

Availability of data and material None.

Ethics approval The authors confirm that there were no ethical in preparing this manuscript.

Consent to participate All authors consent to participating in this work.

Consent for publication All authors consent to publishing this work.

References

Abitbol T, Marway H, Cranston Emily D (2014) Surface modification of cellulose nanocrystals with cetyltrimethylammonium bromide. Nord Pulp Pap Res J 29(1):46. https://doi.org/10.3183/npprj-2014-29-01-p046-057

Ahmadi M, Behzad T, Bagheri R, Ghiaci M, Sain M (2017) Topochemistry of cellulose nanofibers resulting from molecular and polymer grafting. Cellulose 24(5):2139–2152. https://doi.org/10.1007/s10570-017-1254-5

Anžlovar A, Huskić M, Žagar E (2016) Modification of nanocrystalline cellulose for application as a reinforcing nanofiller in PMMA composites. Cellulose 23(1):505–518

Arteta SM, Vera R, Pérez LD (2017) Hydrophobic cellulose fibers via ATRP and their performance in the removal of pyrene from water. J Appl Polym Sci 134(7):444821–444828. https://doi.org/10.1002/app.44482

Atalla RH, Gast J, Sindorf D, Bartuska V, Maciel G (1980) Carbon-13 NMR spectra of cellulose polymorphs. J Am Chem Soc 102(9):3249–3251

Balasubramaniam SL, Patel AS, Nayak B (2020) Surface modification of cellulose nanofiber film with fatty acids for developing renewable hydrophobic food packaging. Food Packag Shelf Life 26(100587):1–9. https://doi.org/10.1016/j.fpsl.2020.100587

Bao X, Fan X, Yu Y, Wang Q, Wang P, Yuan J (2020) Graft modification of lignin-based cellulose via enzyme-initiated reversible addition-fragmentation chain transfer (RAFT) polymerization and free-radical coupling. Int J Biol Macromol 144:267–278. https://doi.org/10.1016/j.ijbiomac.2019.12.078

Barsbay M, Güven O, Stenzel MH, Davis TP, Barner-Kowollik C, Barner L (2007) Verification of controlled grafting of styrene from cellulose via radiation-induced RAFT polymerization. Macromolecules 40(20):7140–7147. https://doi.org/10.1021/ma070825u

Bongiovanni R, Zeno E, Pollicino A, Serafini PM, Tonelli C (2011) UV light-induced grafting of fluorinated monomer onto cellulose sheets. Cellulose 18(1):117–126. https://doi.org/10.1007/s10570-010-9451-5

Boujemaoui A, Mazières S, Malmström E, Destarac M, Carlmark A (2016) SI-RAFT/MADIX polymerization of

vinyl acetate on cellulose nanocrystals for nanocomposite applications. Polymer 99:240–249. https://doi.org/10.1016/j.polymer.2016.07.013

Braunecker WA, Matyjaszewski K (2007) Controlled/living radical polymerization: features, developments, and perspectives. Prog Polym Sci 32(1):93–146. https://doi.org/10.1016/j.progpolymsci.2006.11.002

Cao X, Habibi Y, Lucia LA (2009) One-pot polymerization, surface grafting, and processing of waterborne polyurethane-cellulose nanocrystal nanocomposites. J Mater Chem 19(38):7137–7145. https://doi.org/10.1039/B910517D

Carlmark A, Malmström E (2002) Atom transfer radical polymerization from cellulose fibers at ambient temperature. J Am Chem Soc 124(6):900–901. https://doi.org/10.1021/ja016582h

Carlmark A, Larsson E, Malmström E (2012) Grafting of cellulose by ring-opening polymerisation—a review. Eur Polym J 48(10):1646–1659. https://doi.org/10.1016/j.eurpolymj.2012.06.013

Çetin NS, Tingaut P, Özmen N, Henry N, Harper D, Dadmun M, Sèbe G (2009) Acetylation of cellulose nanowhiskers with vinyl acetate under moderate conditions. Macromol Biosci 9(10):997–1003. https://doi.org/10.1002/mabi.200900073

Charleux B, Nicolas J, Guerret O (2005) Theoretical expression of the average activation—deactivation equilibrium constant in controlled/living free-radical copolymerization operating via reversible termination. Application to a strongly improved control in nitroxide-mediated polymerization of methyl methacrylate. Macromolecules 38(13):5485–5492. https://doi.org/10.1021/ma050087e

Chen H (2014) Chemical composition and structure of natural lignocellulose. In: Chen H (ed) Biotechnology of lignocellulose: theory and practice, edn. Springer, Netherlands, pp 25–71

Chen G, Dufresne A, Huang J, Chang PR (2009) A novel thermoformable bionanocomposite based on cellulose nanocrystal-graft-poly(ε-caprolactone). Macromol Mater Eng 294(1):59–67. https://doi.org/10.1002/mame.200800261

Couturaud B, Baldo A, Mas A, Robin JJ (2015) Improvement of the interfacial compatibility between cellulose and poly(l-lactide) films by plasma-induced grafting of l-lactide: the evaluation of the adhesive properties using a peel test. J Colloid Interface Sci 448:427–436. https://doi.org/10.1016/j.jcis.2015.02.035

Cunha AG, Gandini A (2010) Turning polysaccharides into hydrophobic materials: a critical review. Part 1. Cellulose. Cellulose 17(5):875–889. https://doi.org/10.1007/s10570-010-9434-6

Cvelbar U, Walsh JL, Černák M, de Vries HW, Reuter S, Belmonte T, Corbella C, Miron C, Hojnik N, Jurov A, Puliyalil H, Gorjanc M, Portal S, Laurita R, Colombo V, Schäfer J, Nikiforov A, Modic M, Kylian O, Polak M, Labay C, Canal JM, Canal C, Gherardi M, Bazaka K, Sonar P, Ostrikov KK, Cameron D, Thomas S, Weltmann K-D (2019) White paper on the future of plasma science and technology in plastics and textiles. Plasma Process Polym 16(1):17002281–17002337. https://doi.org/10.1002/ppap.201700228

Dankovich TA, Gray DG (2011) Contact angle measurements on smooth nanocrystalline cellulose (I) thin films. J Adhes Sci Technol 25(6–7):699–708. https://doi.org/10.1163/016942410X525885

Desmet G, Takács E, Wojnárovits L, Borsa J (2011) Cellulose functionalization via high-energy irradiation-initiated grafting of glycidyl methacrylate and cyclodextrin immobilization. Radiat Phys Chem 80(12):1358–1362. https://doi.org/10.1016/j.radphyschem.2011.07.009

Dimitrakellis P, Gogolides E (2018) Hydrophobic and superhydrophobic surfaces fabricated using atmospheric pressure cold plasma technology: A review. Adv Coll Interface Sci 254:1–21. https://doi.org/10.1016/j.cis.2018.03.009

EU (2019) Directive (EU) 2019/904: directive on single-use plastics. Directive (EU) 2019/904. European Parliament and the Council of the European Union

Dizge N, Shaulsky E, Karanikola V (2019) Electrospun cellulose nanofibers for superhydrophobic and oleophobic membranes. J Membr Sci 590(117271):1–9. https://doi.org/10.1016/j.memsci.2019.117271

Dufresne A (2013) Nanocellulose: from nature to high performance tailored materials. De Gruyter

Eissa AM, Khosravi E, Cimecioglu AL (2012) A versatile method for functionalization and grafting of 2-hydroxyethyl cellulose (HEC) via Click chemistry. Carbohyd Polym 90(2):859–869. https://doi.org/10.1016/j.carbpol.2012.06.012

Eksiler K, Andou Y, Shirai Y (2018) Simple manufacture of surface-modified nanolignocellulose fiber via vapor-phase-assisted surface polymerization. ACS Omega 3(4):4545–4550. https://doi.org/10.1021/acsomega.8b00338

Emami Z, Meng Q, Pircheraghi G, Manas-Zloczower I (2015) Use of surfactants in cellulose nanowhisker/epoxy nanocomposites: effect on filler dispersion and system properties. Cellulose 22(5):3161–3176. https://doi.org/10.1007/s10570-015-0728-6

Espino-Pérez E, Gilbert RG, Domenek S, Brochier-Salon MC, Belgacem MN, Bras J (2016) Nanocomposites with functionalised polysaccharide nanocrystals through aqueous free radical polymerisation promoted by ozonolysis. Carbohyd Polym 135:256–266. https://doi.org/10.1016/j.carbpol.2015.09.005

Felix JM, Gatenholm P, Schreiber HP (1993) Controlled interactions in cellulose-polymer composites. 1: effect on mechanical properties. Polym Compos 14(6):449–457. https://doi.org/10.1002/pc.750140602

Fleet R, McLeary JB, Grumel V, Weber WG, Matahwa H, Sanderson RD (2008) RAFT mediated polysaccharide copolymers. Eur Polym J 44(9):2899–2911. https://doi.org/10.1016/j.eurpolymj.2008.06.042

Forsman N, Lozhechnikova A, Khakalo A, Johansson L-S, Vartiainen J, Österberg M (2017) Layer-by-layer assembled hydrophobic coatings for cellulose nanofibril films and textiles, made of polylysine and natural wax particles. Carbohyd Polym 173:392–402. https://doi.org/10.1016/j.carbpol.2017.06.007

Forsman N, Johansson L-S, Koivula H, Tuure M, Kääriäinen P, Österberg M (2020) Open coating with natural wax particles enables scalable, non-toxic hydrophobation of

cellulose-based textiles. Carbohyd Polym 227:115363. https://doi.org/10.1016/j.carbpol.2019.115363
Fu Y, Li G, Yu H, Liu Y (2012) Hydrophobic modification of wood via surface-initiated ARGET ATRP of MMA. Appl Surf Sci 258(7):2529–2533. https://doi.org/10.1016/j.apsusc.2011.10.087
Garcia-Valdez O, Brescacin T, Arredondo J, Bouchard J, Jessop PG, Champagne P, Cunningham MF (2017) Grafting CO2-responsive polymers from cellulose nanocrystals via nitroxide-mediated polymerisation. Polym Chem 8(28):4124–4131. https://doi.org/10.1039/C7PY00631D
Garnett JL, Ng L-T, Viengkhou V (1999) Grafting of methyl methacrylate to cellulose and polypropylene with UV and ionising radiation in the presence of additives including CT complexes. Radiat Phys Chem 56(4):387–403. https://doi.org/10.1016/S0969-806X(99)00327-8
Goffin A-L, Raquez J-M, Duquesne E, Siqueira G, Habibi Y, Dufresne A, Dubois P (2011) From interfacial ring-opening polymerization to melt processing of cellulose nanowhisker-filled polylactide-based nanocomposites. Biomacromology 12(7):2456–2465. https://doi.org/10.1021/bm200581h
Grygiel K, Wicklein B, Zhao Q, Eder M, Pettersson T, Bergström L, Antonietti M, Yuan J (2014) Omnidispersible poly(ionic liquid)-functionalized cellulose nanofibrils: surface grafting and polymer membrane reinforcement. Chem Commun 50(83):12486–12489. https://doi.org/10.1039/C4CC04683H
Guo J, Du W, Gao Y, Cao Y, Yin Y (2017) Cellulose nanocrystals as water-in-oil Pickering emulsifiers via intercalative modification. Colloids Surf A 529:634–642. https://doi.org/10.1016/j.colsurfa.2017.06.056
Gupta KC, Sahoo S, Khandekar K (2002) Graft copolymerization of ethyl acrylate onto cellulose using ceric ammonium nitrate as initiator in aqueous medium. Biomacromology 3(5):1087–1094. https://doi.org/10.1021/bm020060s
Gustafsson E, Larsson PA, Wågberg L (2012) Treatment of cellulose fibres with polyelectrolytes and wax colloids to create tailored highly hydrophobic fibrous networks. Colloids Surf A 414:415–421. https://doi.org/10.1016/j.colsurfa.2012.08.042
Habibi Y (2014) Key advances in the chemical modification of nanocelluloses. Chem Soc Rev 43(5):1519–1542. https://doi.org/10.1039/C3CS60204D
Habibi Y, Dufresne A (2008) Highly filled bionanocomposites from functionalized polysaccharide nanocrystals. Biomacromology 9(7):1974–1980. https://doi.org/10.1021/bm8001717
Habibi Y, Goffin A-L, Schiltz N, Duquesne E, Dubois P, Dufresne A (2008) Bionanocomposites based on poly(ε-caprolactone)-grafted cellulose nanocrystals by ring-opening polymerization. J Mater Chem 18(41):5002–5010. https://doi.org/10.1039/B809212E
Habibi Y, Aouadi S, Raquez J-M, Dubois P (2013) Effects of interfacial stereocomplexation in cellulose nanocrystal-filled polylactide nanocomposites. Cellulose 20(6):2877–2885. https://doi.org/10.1007/s10570-013-0058-5
Hafrén J, Córdova A (2005) Direct organocatalytic polymerization from cellulose fibers. Macromol Rapid Commun 26(2):82–86. https://doi.org/10.1002/marc.200400470
Hansson S, Östmark E, Carlmark A, Malmström E (2009) ARGET ATRP for versatile grafting of cellulose using various monomers. ACS Appl Mater Interfaces 1(11):2651–2659. https://doi.org/10.1021/am900547g
Harrisson S, Drisko GL, Malmström E, Hult A, Wooley KL (2011) Hybrid rigid/soft and biologic/synthetic materials: polymers grafted onto cellulose microcrystals. Biomacromology 12(4):1214–1223. https://doi.org/10.1021/bm101506j
Huang C-F, Chen J-K, Tsai T-Y, Hsieh Y-A, Andrew Lin K-Y (2015) Dual-functionalized cellulose nanofibrils prepared through TEMPO-mediated oxidation and surface-initiated ATRP. Polymer 72:395–405. https://doi.org/10.1016/j.polymer.2015.02.056
Hubbe MA, Rojas OJ, Lucia LA (2015) Green modification of surface characteristics of cellulosic materials at the molecular or nano scale: a review. BioResources 10(3):6095–6206
Jadhav AC, Jadhav NC (2021) Graft copolymerization of methyl methacrylate on Abelmoschus manihot fibres and their application in oil absorbency. Polym Bull 78(7):3913–3941. https://doi.org/10.1007/s00289-020-03308-y
Jarvis MC (2018) Structure of native cellulose microfibrils, the starting point for nanocellulose manufacture. Philos Trans R Soc Math Phys Eng Sci 376(2112):20170045. https://doi.org/10.1098/rsta.2017.0045
Kalantari M, Du R, Ayranci C, Boluk Y (2018) Effects of interfacial interactions and interpenetrating brushes on the electrospinning of cellulose nanocrystals-polystyrene fibers. J Colloid Interface Sci 528:419–430. https://doi.org/10.1016/j.jcis.2018.04.089
Kan KHM, Li J, Wijesekera K, Cranston ED (2013) Polymer-grafted cellulose nanocrystals as ph-responsive reversible flocculants. Biomacromology 14(9):3130–3139. https://doi.org/10.1021/bm400752k
Kedzior SA, Graham L, Moorlag C, Dooley BM, Cranston ED (2016) Poly(methyl methacrylate)-grafted cellulose nanocrystals: one-step synthesis, nanocomposite preparation, and characterization. Can J Chem Eng 94(5):811–822. https://doi.org/10.1002/cjce.22456
Kedzior SA, Zoppe JO, Berry RM, Cranston ED (2019) Recent advances and an industrial perspective of cellulose nanocrystal functionalization through polymer grafting. Curr Opin Solid State Mater Sci 23(2):74–91. https://doi.org/10.1016/j.cossms.2018.11.005
Kelly PV, Cheng P, Gardner DJ, Gramlich WM (2021) Aqueous polymer modification of cellulose nanofibrils by grafting-through a reactive methacrylate group. Macromol Rapid Commun 42(3):2000531. https://doi.org/10.1002/marc.202000531
Khan F (2005) Characterization of methyl methacrylate grafting onto preirradiated biodegradable lignocellulose fiber by γ-radiation. Macromol Biosci 5(1):78–89. https://doi.org/10.1002/mabi.200400137
Klemm D, Kramer F, Moritz S, Lindström T, Ankerfors M, Gray D, Dorris A (2011) Nanocelluloses: A New Family of Nature-Based Materials. Angew Chem Int Ed

50(24):5438–5466. https://doi.org/10.1002/anie.201001273

Krouit M, Bras J, Belgacem MN (2008) Cellulose surface grafting with polycaprolactone by heterogeneous click-chemistry. Eur Polymer J 44(12):4074–4081. https://doi.org/10.1016/j.eurpolymj.2008.09.016

Lacerda PSS, Barros-Timmons AMMV, Freire CSR, Silvestre AJD, Neto CP (2013) Nanostructured composites obtained by ATRP sleeving of bacterial cellulose nanofibers with acrylate polymers. Biomacromology 14(6):2063–2073. https://doi.org/10.1021/bm400432b

Laitinen O, Suopajärvi T, Österberg M, Liimatainen H (2017) Hydrophobic, superabsorbing aerogels from choline chloride-based deep eutectic solvent pretreated and silylated cellulose nanofibrils for selective oil removal. ACS Appl Mater Interfaces 9(29):25029–25037. https://doi.org/10.1021/acsami.7b06304

Li G, Zheng H, Wang Y, Wang H, Dong Q, Bai R (2010a) A facile strategy for the fabrication of highly stable superhydrophobic cotton fabric using amphiphilic fluorinated triblock azide copolymers. Polymer 51(9):1940–1946. https://doi.org/10.1016/j.polymer.2010.03.002

Li ZQ, Zhou XD, Pei CH (2010b) Synthesis of PLA-co-PGMA copolymer and its application in the surface modification of bacterial cellulose. Int J Polym Mater Polym Biomater 59(9):725–737. https://doi.org/10.1080/00914037.2010.483214

Li SH, Huang JY, Ge MZ, Li SW, Xing TL, Chen GQ, Liu YQ, Zhang KQ, Al-Deyab SS, Lai YK (2015) Controlled grafting superhydrophobic cellulose surface with environmentally-friendly short fluoroalkyl chains by ATRP. Mater Des 85:815–822. https://doi.org/10.1016/j.matdes.2015.07.083

Lin N, Chen G, Huang J, Dufresne A, Chang PR (2009) Effects of polymer-grafted natural nanocrystals on the structure and mechanical properties of poly(lactic acid): a case of cellulose whisker-graft-polycaprolactone. J Appl Polym Sci 113(5):3417–3425. https://doi.org/10.1002/app.30308

Lindqvist J, Nyström D, Östmark E, Antoni P, Carlmark A, Johansson M, Hult A, Malmström E (2008) Intelligent dual-responsive cellulose surfaces via surface-initiated ATRP. Biomacromology 9(8):2139–2145. https://doi.org/10.1021/bm800193n

Lingström R, Notley SM, Wågberg L (2007) Wettability changes in the formation of polymeric multilayers on cellulose fibres and their influence on wet adhesion. J Colloid Interface Sci 314(1):1–9. https://doi.org/10.1016/j.jcis.2007.04.046

Littunen K, Hippi U, Johansson L-S, Österberg M, Tammelin T, Laine J, Seppälä J (2011) Free radical graft copolymerization of nanofibrillated cellulose with acrylic monomers. Carbohyd Polym 84(3):1039–1047. https://doi.org/10.1016/j.carbpol.2010.12.064

Lizundia E, Fortunati E, Dominici F, Vilas JL, León LM, Armentano I, Torre L, Kenny JM (2016) PLLA-grafted cellulose nanocrystals: Role of the CNC content and grafting on the PLA bionanocomposite film properties. Carbohyd Polym 142:105–113. https://doi.org/10.1016/j.carbpol.2016.01.041

Lönnberg H, Zhou Q, Brumer H, Teeri TT, Malmström E, Hult A (2006) Grafting of cellulose fibers with poly(ε-caprolactone) and poly(l-lactic acid) via ring-opening polymerization. Biomacromology 7(7):2178–2185. https://doi.org/10.1021/bm060178z

Lönnberg H, Fogelström L, Berglund L, Malmström E, Hult A (2008) Surface grafting of microfibrillated cellulose with poly(ε-caprolactone)—synthesis and characterization. Eur Polym J 44(9):2991–2997. https://doi.org/10.1016/j.eurpolymj.2008.06.023

Lorandi F, Matyjaszewski K (2020) Why do we need more active ATRP catalysts? Isr J Chem 60(1–2):108–123. https://doi.org/10.1002/ijch.201900079

Maatar W, Boufi S (2015) Poly(methacylic acid-co-maleic acid) grafted nanofibrillated cellulose as a reusable novel heavy metal ions adsorbent. Carbohyd Polym 126:199–207. https://doi.org/10.1016/j.carbpol.2015.03.015

Madrid JF, Abad LV (2015) Modification of microcrystalline cellulose by gamma radiation-induced grafting. Radiat Phys Chem 115:143–147. https://doi.org/10.1016/j.radphyschem.2015.06.025

Margutti S, Vicini S, Proietti N, Capitani D, Conio G, Pedemonte E, Segre AL (2002) Physical–chemical characterisation of acrylic polymers grafted on cellulose. Polymer 43(23):6183–6194. https://doi.org/10.1016/S0032-3861(02)00533-5

Matyjaszewski Polymer Group (2021) Atom transfer radical polymerization (ATRP). Retrieved 22.10.2021, from https://www.cmu.edu/maty/chem/fundamentals-atrp/atrp.html

Medronho B, Lindman B (2014) Competing forces during cellulose dissolution: From solvents to mechanisms. Curr Opin Colloid Interface Sci 19(1):32–40. https://doi.org/10.1016/j.cocis.2013.12.001

Misra BN, Dogra R, Kaur I, Jassal JK (1979) Grafting onto cellulose. IV. Effect of complexing agents on Fenton's reagent (Fe2+-H2O2)-initiated grafting of poly(vinyl acetate). J Polym Sci Polym Chem Edn 17(6):1861–1863. https://doi.org/10.1002/pol.1979.170170631

Misra BN, Dogra R, Mehta IK (1980) Grafting onto cellulose. V. Effect of complexing agents on Fenton's reagent (Fe2+−H2O2) -initiated grafting of poly(ethyl acrylate). J Polym Sci Polym Chem Edn 18(2):749–752. https://doi.org/10.1002/pol.1980.170180234

Moad G, Rizzardo E, Thang SH (2005) Living radical polymerization by the RAFT process. Aust J Chem 58(6):379–410

Mondal MIH, Uraki Y, Ubukata M, Itoyama K (2008) Graft polymerization of vinyl monomers onto cotton fibres pretreated with amines. Cellulose 15(4):581–592. https://doi.org/10.1007/s10570-008-9210-z

Morandi G, Heath L, Thielemans W (2009) Cellulose nanocrystals grafted with polystyrene chains through surface-initiated atom transfer radical polymerization (SI-ATRP). Langmuir 25(14):8280–8286. https://doi.org/10.1021/la900452a

Moreira G, Fedeli E, Ziarelli F, Capitani D, Mannina L, Charles L, Viel S, Gigmes D, Lefay C (2015) Synthesis of polystyrene-grafted cellulose acetate copolymers via nitroxide-mediated polymerization. Polym Chem 6(29):5244–5253. https://doi.org/10.1039/C5PY00752F

Mulyadi A, Zhang Z, Deng Y (2016) Fluorine-free oil absorbents made from cellulose nanofibril aerogels. ACS Appl Mater Interfaces 8(4):2732–2740. https://doi.org/10.1021/acsami.5b10985

Nagalakshmaiah M, Pignon F, El Kissi N, Dufresne A (2016) Surface adsorption of triblock copolymer (PEO–PPO–PEO) on cellulose nanocrystals and their melt extrusion with polyethylene. RSC Adv 6(70):66224–66232. https://doi.org/10.1039/C6RA11139D

Nicolas J, Dire C, Mueller L, Belleney J, Charleux B, Marque SRA, Bertin D, Magnet S, Couvreur L (2006) Living character of polymer chains prepared via nitroxide-mediated controlled free-radical polymerization of methyl methacrylate in the presence of a small amount of styrene at low temperature. Macromolecules 39(24):8274–8282. https://doi.org/10.1021/ma061380x

Nicolas J, Brusseau S, Charleux B (2010) A minimal amount of acrylonitrile turns the nitroxide-mediated polymerization of methyl methacrylate into an almost ideal controlled/living system. J Polym Sci A Polym Chem 48(1):34–47. https://doi.org/10.1002/pola.23749

Nicolas J, Guillaneuf Y, Lefay C, Bertin D, Gigmes D, Charleux B (2013) Nitroxide-mediated polymerization. Prog Polym Sci 38(1):63–235. https://doi.org/10.1016/j.progpolymsci.2012.06.002

Nurmi L, Kontturi K, Houbenov N, Laine J, Ruokolainen J, Seppälä J (2010) Modification of surface wettability through adsorption of partly fluorinated statistical and block polyelectrolytes from aqueous medium. Langmuir 26(19):15325–15332. https://doi.org/10.1021/la1023345

Nyström D, Lindqvist J, Östmark E, Hult A, Malmström E (2006) Superhydrophobic bio-fibre surfaces via tailored grafting architecture. Chem Commun 34:3594–3596. https://doi.org/10.1039/B607411A

Odian G (2004) Radical chain polymerization, principles of polymerization, 4th edn. Wiley, New Jersey, pp 198–349

Ogawa T, Ding B, Sone Y, Shiratori S (2007) Super-hydrophobic surfaces of layer-by-layer structured film-coated electrospun nanofibrous membranes. Nanotechnology 18(16):1656071–1656078. https://doi.org/10.1088/0957-4484/18/16/165607

Ogiwara Y, Kubota H (1973) Photo-induced radical formation in cellulose. J Polym Sci Polym Chem Edn 11(12):3243–3253. https://doi.org/10.1002/pol.1973.170111217

Olsén P, Herrera N, Berglund LA (2020) Polymer grafting inside wood cellulose fibers by improved hydroxyl accessibility from fiber swelling. Biomacromology 21(2):597–603. https://doi.org/10.1021/acs.biomac.9b01333

Parida D, Jassal M, Agarwal AK (2012) Functionalization of cotton by in-situ reaction of styrene in atmospheric pressure plasma zone. Plasma Chem Plasma Process 32(6):1259–1274

Pei A, Malho J-M, Ruokolainen J, Zhou Q, Berglund LA (2011) Strong nanocomposite reinforcement effects in polyurethane elastomer with low volume fraction of cellulose nanocrystals. Macromolecules 44(11):4422–4427. https://doi.org/10.1021/ma200318k

Perrier S, Takolpuckdee P, Westwood J, Lewis DM (2004) Versatile chain transfer agents for reversible addition fragmentation chain transfer (RAFT) polymerization to synthesize functional polymeric architectures. Macromolecules 37(8):2709–2717. https://doi.org/10.1021/ma035468b

Purushotham P, Ho R, Zimmer J (2020) Architecture of a catalytically active homotrimeric plant cellulose synthase complex. Science 369(6507):1089–1094. https://doi.org/10.1126/science.abb2978

Rechendorff K, Hovgaard MB, Foss M, Zhdanov VP, Besenbacher F (2006) Enhancement of protein adsorption induced by surface roughness. Langmuir 22(26):10885–10888. https://doi.org/10.1021/la0621923

Rodionova G, Lenes M, Eriksen Ø, Gregersen Ø (2011) Surface chemical modification of microfibrillated cellulose: improvement of barrier properties for packaging applications. Cellulose 18(1):127–134. https://doi.org/10.1007/s10570-010-9474-y

Rodríguez-Fabià S, Torstensen J, Johansson L, Syverud K (2022) Hydrophobisation of lignocellulosic materials part I: physical modification. Cellulose 29(10): 5375–5393. https://doi.org/10.1007/s10570-022-04620-8

Roy D, Guthrie JT, Perrier S (2005) Graft polymerization: grafting poly(styrene) from cellulose via reversible addition−fragmentation chain transfer (RAFT) polymerization. Macromolecules 38(25):10363–10372. https://doi.org/10.1021/ma0515026

Roy D, Semsarilar M, Guthrie JT, Perrier S (2009) Cellulose modification by polymer grafting: a review. Chem Soc Rev 38(7):2046–2064. https://doi.org/10.1039/B808639G

Sakakibara K, Yano H, Tsujii Y (2016) Surface engineering of cellulose nanofiber by adsorption of diblock copolymer dispersant for green nanocomposite materials. ACS Appl Mater Interfaces 8(37):24893–24900. https://doi.org/10.1021/acsami.6b07769

Samanta KK, Joshi AG, Jassal M, Agrawal AK (2012) Study of hydrophobic finishing of cellulosic substrate using He/1,3-butadiene plasma at atmospheric pressure. Surf Coat Technol 213:65–76. https://doi.org/10.1016/j.surfcoat.2012.10.016

Sciannamea V, Jérôme R, Detrembleur C (2008) In-situ nitroxide-mediated radical polymerization (NMP) processes: their understanding and optimization. Chem Rev 108(3):1104–1126. https://doi.org/10.1021/cr0680540

Sharmin N, Khan RA, Salmieri S, Dussault D, Bouchard J, Lacroix M (2012) Modification and characterization of biodegradable methylcellulose films with trimethylolpropane trimethacrylate (TMPTMA) by γ radiation: effect of nanocrystalline cellulose. J Agric Food Chem 60(2):623–629. https://doi.org/10.1021/jf203500s

Shukla SR, Athalye AR (1994) Graft-copolymerization of glycidyl methacrylate onto cotton cellulose. J Appl Polym Sci 54(3):279–288. https://doi.org/10.1002/app.1994.070540302

Shukla SR, Rao GVG, Athalye AR (1993) Improving graft level during photoinduced graft-copolymerization of styrene onto cotton cellulose. J Appl Polym Sci 49(8):1423–1430. https://doi.org/10.1002/app.1993.070490810

Stenstad P, Andresen M, Tanem BS, Stenius P (2008) Chemical surface modifications of microfibrillated cellulose. Cellulose 15(1):35–45. https://doi.org/10.1007/s10570-007-9143-y

Tang W, Huang Y, Meng W, Qing F-L (2010) Synthesis of fluorinated hyperbranched polymers capable as highly hydrophobic and oleophobic coating materials. Eur Polym J 46(3):506–518. https://doi.org/10.1016/j.eurpolymj.2009.12.005

Tastet D, Save M, Charrier F, Charrier B, Ledeuil J-B, Dupin J-C, Billon L (2011) Functional biohybrid materials synthesized via surface-initiated MADIX/RAFT polymerization from renewable natural wood fiber: grafting of polymer as non leaching preservative. Polymer 52(3):606–616. https://doi.org/10.1016/j.polymer.2010.12.046

Thakur VK, Singha AS (2010) KPS-initiated graft copolymerization onto modified cellulosic biofibers. Int J Polym Anal Charact 15(8):471–485. https://doi.org/10.1080/1023666X.2010.510294

Thakur VK, Singha AS, Misra BN (2011) Graft copolymerization of methyl methacrylate onto cellulosic biofibers. J Appl Polym Sci 122(1):532–544. https://doi.org/10.1002/app.34094

Tosh B, Routray CR (2014) Grafting of cellulose based materials: a review. Chem Sci Rev Lett 3(10):74–92

Verma SK, Kaur I (2012) Gamma-induced polymerization and grafting of a novel phosphorous-, nitrogen-, and sulfur-containing monomer on cotton fabric to impart flame retardancy. J Appl Polym Sci 125(2):1506–1512. https://doi.org/10.1002/app.36340

Vidiella del Blanco M, Gomez V, Keplinger T, Cabane E, Morales LFG (2019) Solvent-controlled spatial distribution of SI-AGET-ATRP grafted polymers in lignocellulosic materials. Biomacromology 20(1):336–346. https://doi.org/10.1021/acs.biomac.8b01393

Wang J, Siqueira G, Müller G, Rentsch D, Huch A, Tingaut P, Levalois-Grützmacher J, Grützmacher H (2016) Synthesis of new bis(acyl)phosphane oxide photoinitiators for the surface functionalization of cellulose nanocrystals. Chem Commun 52(13):2823–2826. https://doi.org/10.1039/C5CC09760F

Wei DW, Wei H, Gauthier AC, Song J, Jin Y, Xiao H (2020) Superhydrophobic modification of cellulose and cotton textiles: Methodologies and applications. J Bioresour Bioprod 5(1):1–15. https://doi.org/10.1016/j.jobab.2020.03.001

Yang H, Deng Y (2008) Preparation and physical properties of superhydrophobic papers. J Colloid Interface Sci 325(2):588–593. https://doi.org/10.1016/j.jcis.2008.06.034

Yang Q, Pan X, Huang F, Li K (2011) Synthesis and characterization of cellulose fibers grafted with hyperbranched poly(3-methyl-3-oxetanemethanol). Cellulose 18(6):1611–1621. https://doi.org/10.1007/s10570-011-9587-y

Yang J, Pu Y, Miao D, Ning X (2018) Fabrication of durably superhydrophobic cotton fabrics by atmospheric pressure plasma treatment with a siloxane precursor. Polymers 10(4):460. https://doi.org/10.3390/polym10040460

Yang X, Ku T-H, Biswas SK, Yano H, Abe K (2019) UV grafting: surface modification of cellulose nanofibers without the use of organic solvents. Green Chem 21(17):4619–4624. https://doi.org/10.1039/C9GC02035G

Yi J, Xu Q, Zhang X, Zhang H (2008) Chiral-nematic self-ordering of rodlike cellulose nanocrystals grafted with poly(styrene) in both thermotropic and lyotropic states. Polymer 49(20):4406–4412. https://doi.org/10.1016/j.polymer.2008.08.008

Yu H-Y, Qin Z-Y (2014) Surface grafting of cellulose nanocrystals with poly(3-hydroxybutyrate-co-3-hydroxyvalerate). Carbohyd Polym 101:471–478. https://doi.org/10.1016/j.carbpol.2013.09.048

Zhang Q, Jiang Y, Yao L, Jiang Q, Qiu Y (2015) Hydrophobic surface modification of ramie fibers by plasma-induced addition polymerization of propylene. J Adhes Sci Technol 29(8):691–704. https://doi.org/10.1080/01694243.2014.997380

Zhou L, He H, Li M-C, Huang S, Mei C, Wu Q (2018) Grafting polycaprolactone diol onto cellulose nanocrystals via click chemistry: Enhancing thermal stability and hydrophobic property. Carbohyd Polym 189:331–341. https://doi.org/10.1016/j.carbpol.2018.02.039

Zhu L, Chen Q, Wang Y, Huang H, Luo W, Li Z, Zhang Z, Hadjichristidis N (2021) Grafting polysulfonamide from cellulose paper through organocatalytic ring-opening polymerization of N-sulfonyl aziridines. Carbohyd Polym 261:117903. https://doi.org/10.1016/j.carbpol.2021.117903

Zhuo J, Sun G (2014) Light-induced surface graft polymerizations initiated by an anthraquinone dye on cotton fibers. Carbohyd Polym 112:158–164. https://doi.org/10.1016/j.carbpol.2014.05.084

Zoppe JO, Dupire AVM, Lachat TGG, Lemal P, Rodriguez-Lorenzo L, Petri-Fink A, Weder C, Klok H-A (2017) Cellulose nanocrystals with tethered polymer chains: chemically patchy versus uniform decoration. ACS Macro Lett 6(9):892–897. https://doi.org/10.1021/acsmacrolett.7b00383